CHAPTER

1

1. Introduction

Fluid Mechanics is the study of fluids either at rest (fluids static) or in motion (fluids dynamics and kinematics) and the subsequent effects of the fluids upon the boundaries which may be either solid surfaces or interfaces with other fluids. It is worth noting that both gases and liquids are classified as fluids according to Batchelor [8]. Fluids, unlike solids, lack ability to offer sustained resistance to a deforming force. Thus, a fluid is a substance which deforms continuously under the action of shearing forces, however small they may be. Deformation is caused by shearing forces - forces that act tangentially to the surfaces to which they are applied according to Douglas et al. [23].

1.1 Definition of Terms [8, 55]

Some relevant fluid properties to be considered in this study are highlighted as follows:

Pressure

Pressure is the stress at a point in a static fluid. Gradient in pressure often drives a fluid flow, especially in ducts. The unit is N m^{-2}

Temperature

This is the measure of internal energy of a fluid. If the temperature differences are strong, heat transfer may be important. The unit is degree Celsius (^{o}C).

Density

The density of a fluid is its mass per unit volume. Density in liquids is nearly constant. This property aids the classification of fluids as either compressible or incompressible. A fluid is termed compressible if its density varies and increases nearly proportionally to the pressure level. Otherwise it is termed incompressible according to White [55]. The unit of density is kgm^{-3}.

Internal Energy

In thermo-statics the only energy in a substance is that stored in a system by molecular activity and molecular bonding forces. This is commonly denoted as internal energy. An identified mass of viscous fluid may be viewed as a thermodynamic system that stores various forms of energy. Whenever any form of this fluid is being deformed there results an irreversible transformation of mechanical energy into internal or thermal energy. The internal energy of gas includes the energies of translation, rotation and vibration of the molecules as well as energy of molecular dissociation and energy of electronic excitation of the molecules. The unit is J mol^{-1}.

Specific Heat Capacity

This refers to the measure of the heat energy required to raise the temperature of one gram of a substance by one degree Celsius. There are two distinctly different experimental conditions under which specific heat capacity is measured. It is measured

either under constant pressure condition or under constant volume condition. Typical values of the specific heat of gases are not much different from those of liquids. The unit is J $mol^{-1} K^{-1}$.

Thermal Conductivity

This is the property of fluid that relates the vector rate of heat flow per unit area to the vector gradient of temperature. This proportionality observed experimentally for fluids and solids, is known as Fourier's law of heat conduction.

$q = -k\nabla T$.

The minus sign satisfies the convection that heat flux is positive in the direction of decreasing temperature according to Kay and Crawford [34]. The unit is W $m^{-1} K^{-1}$.

Exothermic Reactions

In thermodynamics, the word exothermic "outside heating" describes a process or reaction that releases energy usually in the form of heat, but it can also release energy in form of light (e.g. explosions), sound, or electricity (e.g. a battery). Its etymology stems from the Greek prefix *exo-*, meaning "outside" and the Greek word *thermein*, meaning "to heat". The concept is frequently applied in physical_sciences to chemical_reactions, where chemical bond energy is converted to thermal energy (heat). The energy comes from the bonds that hold the atoms together in the molecules. When these atoms join up during a chemical reaction they all give out a little bit of energy. Because there are millions and millions of molecules the energy they all give out adds up to make heat, a flame or even an explosion. Many fluid materials used in various engineering and industrial processes such as coal slurries, polymer solutions or melts, drilling mud, hydrocarbon oils, grease, etc., are very reactive. Some examples of exothermic processes are [2, 19] :

- Condensation of rain from water vapor
- Combustion of fuels such as coal and oil

- Mixing water and strong acids
- Mixing alkalis and acids
- The setting of cement and concrete
- Most polymerization reactions such as the setting of epoxy resin
- Thermite reaction

Viscosity

A fluid at rest cannot resist shearing forces and if such forces acts in a fluid which is in contact with solid boundary, the fluid will flow over the boundary in such a way that the particles immediately in contact with the boundary have the same velocity as the boundary while successive layers of fluid parallel to the boundary move with increasing velocity. Shear stresses opposing the relative motion of these layers are set up and their magnitude depending on the velocity gradient from layer to layer. For fluids obeying Newton's law of viscosity, taking the direction of motion as the x-direction and U as the velocity of the fluid in the x-direction at a distance y from the boundary, the shear stress in the x-direction is given by [55]

$\tau_x = \mu \frac{dU}{dy}$, where the constant μ is called coefficient of dynamic viscosity

The ratio of the coefficient of dynamic viscosity to mass density is called the kinematic viscosity, υ.

$$\upsilon = \frac{\mu}{\rho}.$$

The viscosity property of fluids aids the classification of fluids into either Newtonian or non-Newtonian fluids. The unit of dynamic viscosity is $kgm^{-1}s^{-1}$.

Viscosity is associated with collective currents that carry momentum from one region of the fluid to another. Consider a fluid where there is, in addition to thermal agitation of the molecules, a collective movement or current of the whole fluid for example, water running in a canal or pipe under a pressure difference. Traditionally viscosity is regarded,

as the most important material property and any practical study that requires the knowledge of fluid response would automatically turn to the basic understanding of viscosity. In general, the Newtonian model describes the rheological behavior of fluids. The Newtonian model is simply a special case with a constant viscosity and viscosity is strong deformation of fluids. It is the key factor in determining the amount of fluid flowing in channels. It also helps to determine whether the flow regime is laminar, transitional or turbulent. Accurate knowledge of viscosity is very useful for computation of the pressure, velocity and temperature within the channels.

Viscosity also helps to describe the flow behavior of shear stress with respect to the rate of deformation of the fluid. In general the application of viscosity includes reservoir modeling, in which production rates and mobility for water flooding plays a major role. Factors that affect viscosity will be discussed in the next section

Temperature-Dependent Viscosity

The effect of increasing the temperature of a fluid is to reduce the cohesive forces while simultaneously increasing the rate of molecular interchange. The former effect tends to cause a decrease of shear stress, while the latter causes it to increase. The net result is that liquid shows a reduction in viscosity with increasing temperature. For instance most lubricants used in automobile have a dynamic viscosity of 0.095Pas at 40^{o}C and 0.0097Pas at 100^{o}C, the operating oil viscosity being taken as 0.015Pas corresponding to an effective operating temperature of 81^{o}C. Shear rate in the lubricant will thus be in the range 4 X 10^{-4} s^{-1} to 1.3 x 10^{-6} s^{-1}. Such shear rates would certainly cause shear thinning effects in a multigrade lubricant [25]. Unlike liquids for which many different temperature-dependent viscosity equations exists only two main laws describes the response of gas viscosity to temperature, they are: power law and Sutherland law. **Table 1.1.1** shows different viscosity models.

Table 1.1.1.: Viscosity-Temperature Equations as in the literature ([21, 23, 34]), a, b, C are constants, T_0 is a reference temperature, μ_0 is the viscosity at T_0 and υ_0 is the kinematic viscosity at T_0 .

NAME	EQUATION
Sutherland	$\mu = \frac{(T/T_0)^{3/2}(T_0 + C)}{T + C}$
Power Law	$\mu = (T/T_0)^n$
Reynolds	$\mu = be^{-aT}$
Slotte	$\mu = \frac{a}{(b+T)^C}$
Walther	$\mu = \mu_0 + bd^{1/T^C}$
Vogel	$\mu = ae^{\frac{b}{T-C}}$
Arrhenius Type	$\mu = \mu_0 \left(\frac{T}{T_0}\right)^n e^{\left(\frac{E}{RT}\right)}$
Williams-Landel-Ferry	$\log\left(\frac{\mu}{\mu_0}\right) = -\frac{C_1(T - T_0)}{C_2 + T - T_0}$

The First Law of Thermodynamics

The first law of thermodynamics is a statement of the conservation of energy. This states that energy can be neither created nor destroyed; it just changes form. The fist law of thermodynamics defines the internal energy as a state function and provides a formal statement of the conservation of energy. However, it provides no information about the direction in which processes can spontaneously occur, that is, the reversibility aspects of thermodynamics processes. For example, it cannot say how cells can perform work while existing in an isothermal environment. It gives no information about the

inability of any thermodynamic processes to convert heat into mechanical work with full efficiency, or any insight into why mixtures cannot spontaneously separate or unmix themselves. An experimentally derived principle to characterize the availability of energy is required to do this. This is precisely the role of the second law of thermodynamics that will be explained next.

The Second Law of Thermodynamics

Although a spontaneous process can proceed only in a definite direction, the first law of thermodynamics gives no information about direction; it merely states that when one form of energy is converted into another, identical quantities of energy are involved regardless of feasibility of the process. In this regard, events could be envisioned that would not violate the first law of thermodynamics, e.g., transfer of certain quantity of heat from a low-temperature body to a high-temperature body, without expenditure of work. However, the reality shows that this is impossible and the first law of thermodynamics becomes inadequate in picturizing the complete energy transfer. Furthermore, experiments indicated that when energy in the form of heat is transferred to a system, only a portion of heat can be converted to work and is usually to converted to work.

The second law of thermodynamics establishes the differences in quality between different forms of energy and explains why some processes can spontaneously occur, whereas other cannot. It indicates a trend of change and is usually expressed as an inequality. The second law of thermodynamics has been confirmed by experimental evidence like other physical laws of nature.

The second law of thermodynamics defines the fundamental physical quantity entropy as a randomized energy state unavailable for direct conversion to work. It also states that all spontaneous processes, both chemical and physical, proceed to maximize entropy, that is, to become more randomized and convert energy into a less available form. A direct consequence of fundamental importance is the implication that at thermodynamic equilibrium the entropy of a system is at a relative maximum; that is, no further increase in disorder is possible without changing by some external means

(such as adding heat) the thermodynamic state of the system. A basic corollary of the second law of thermodynamics is the statement that the sum of the entropy changes of a system and that of the surroundings must always be positive, that is, the universe (the sum of all systems and surroundings) is constrained to become forever more disordered and to proceed towards thermodynamic equilibrium with some absolute maximum value of entropy. From a biological standpoint this is certainly a reasonable concept, since unless gradients in concentration and temperature are forcibly maintained by the consumption of energy, organisms proceed spontaneously towards the biological equivalent of equilibrium-death.

The second law of thermodynamics is quite general. However, when intermolecular forces are long range, as in the case of particles interacting through gravitation, there are difficulties because our classification into extensive variables (proportional to volume) and intensive variables (independent of volume) does not apply. The total energy is no longer proportional to the volume. Fortunately gravitational forces are very weak as compared to the short-range intermolecular forces. It is only on the astrophysical scale that this problem becomes important. The generality of the second law of thermodynamics gives us a powerful means to understand the thermodynamic aspects of real systems through the usage of ideal systems. A classical example is Planck's analysis of radiation in thermodynamic equilibrium with matter (blackbody radiation) in which Planck considered simple harmonic oscillators not merely because they are good approximations of molecules but because the properties of radiation in thermal equilibrium with matter are universal, regardless of the particular nature of the matter with which the radiation interacts. The conclusions one arrives at using idealized oscillators and the laws of thermodynamics must also be valid for all other forms of matter, however complex. What makes this new statement of the second law of thermodynamics valuable as a guide to energy policy is the relationship between entropy and the usefulness of energy. Energy is most useful to us when we can get it to flow from one substance to another, e.g., to warm a house and we can use it to do work. Useful energy thus must have low entropy so that the second law of thermodynamics will allow transfer or conversions to occur spontaneously.

ENTROPY

The thermodynamic irreversibility in any fluid flow process can be quantified through entropy analysis. The first law of thermodynamics is simply an expression of the conservation of energy principle. The second law of thermodynamics states that all real processes are irreversible. Entropy generation is a measure of the account of irreversibility associated with the real processes. As entropy generation takes place, the quality of energy (i.e. exergy) decreases. In order to preserve the quality of energy in a fluid flow process or at least to reduce the entropy generation, it is important to study the distribution of the entropy generation within the fluid volume. The optimal design for any thermal system can be achieved by minimizing entropy generation in the systems. Entropy generation in thermal engineering systems destroys available work and thus reduces its efficiency. Many studies have been published to assess the sources of irreversibility in components and systems. Bejan [9] studied the entropy generation for forced convective heat transfer due to temperature gradient and viscosity effect in a fluid. Bejan [10] also presented various reasons behind entropy generation in applied thermal engineering where the generation of entropy destroys the available work, called exergy, of a system. The general equation for the entropy generation per unit volume is given by;

$$S^m = \frac{k}{T_w^2}(\nabla T)^2 + \frac{\mu}{T_w}\Phi .$$

The first term in the equation is the irreversibility due to heat transfer and the second term is the entropy generation due to viscous dissipation.

Over the past 50 years our view of nature has changed drastically. Classical science emphasized equilibrium and stability. Now we see fluctuations and instability, evolutionary processes on all levels from chemistry and biology to cosmology. Everywhere we observe irreversible processes in which time symmetry is broken. The distinction between reversible and irreversible processes was first introduced in thermodynamics through the concept of “entropy”.

In the modern context the formulation of entropy is for understanding the thermodynamics aspects of self-organization, evolution of order and life that we see in

Nature. When a system is isolated, energy increase will be zero. In this case the entropy of the system will continue to increase due to irreversible processes and reach the maximum possible value, which is the state of thermodynamics equilibrium. In the state of equilibrium, all irreversible processes cease. When the system begins to exchange entropy with the exterior then, in general, it is driven away from equilibrium, and the entropy producing the irreversible processes begins to operate. The exchange of entropy is due to exchange of heat and matter. The entropy flowing out of an adiabatic system is always larger than the entropy flowing into the system, the difference arising due to entropy produced by irreversible processes within the system.

The internal energy of the system is randomly distributed as kinetic energy at the molecular and sub molecular levels and as energy associated with attractive or repulsive forces between molecular and sub molecular entities, which are moving closer together or further apart in relation to the mean separation. This energy is sometimes described as being 'disordered' as it is not accessible as work at the macroscopic level in the same way as is the kinetic energy or gravitational potential energy that an entire system possesses owing to its velocity or position in the gravitational field. Although energy is the capability to do work, it is not possible directly to access the minute quantities of disordered energy possessed at a given instant by the various modes of energy possession of the entities so as to yield mechanical shaft work on the macroscopic scale. The term 'disorder' refers to the lack of information about exactly how much energy is associated at any moment with each mode of energy possession of each molecular or sub molecular entity within the system.

Channel Flow

Channel flow constitutes a very important class of flows in fluid mechanics due to its numerous applications in biological and engineering systems. As a result it is important that we study the characteristics of this flow. We are particularly interested in how the flow pattern is modified by the effects of changing viscosity. The viscosity of many fluids varies with temperature e.g. physiological fluids such as blood, various lubricants used in engineering systems like polymer solutions, mineral oils with polymer

additives, etc. this variation in the fluid viscosity due to temperature certainly affects the flow characteristics. In this respect we shall consider two types of channel flows, namely Poiseuille flow and Couette flow.

Poiseuille flow is flow between two parallel stationary plates due to an imposed constant pressure gradient. Its general characteristic is a parabolic axial velocity profile. Couette flow is considered with the effect of viscosity due to temperature changes on the lubrication that occurs between two moving plates or between a fixed plate and a moving plate.

1.2 Literature Review

The study of flow of a reactive variable viscosity fluid and heat transfer has gained more attention because of its wide applicability in lubrication and tribology, food processing, instrumentation, bio-sciences, lava flows and viscometry. The first viscous fluid flow treated in the classical book by White [55] is the steady flow between a fixed and a moving plate (Couette flow). Unlike Couette flow which is named after Maurice Couette and refers to variety of flows driven by differential tangential motion of enclosing walls, Poiseuille flow is named after J.L.M. Poiseuille and is associated with rectilinear pressure driven flows in stationary conduits. Many research works have been conducted on these two flows (see examples, [3, 11, 22, 24, 36-38]). A large number of reports of investigations has been documented on constant viscosity approximation problems, [2, 11, 39, 40]. Adler [2] investigated the critical values of parameters for steady, reactive, viscous, one-dimensional flow of an incompressible, homogeneous Newtonian fluid between two parallel heated walls. The equations of flow were solved for Bimolecular, Arrhenius and Sensitized temperature dependence cases. It was observed that the critical Frank-Kamenetskii and maximum temperature are decreasing functions of the exponent while transition activation energy parameter is a monotonically increasing function of the exponent.

In the classical system of the thermal boundary layer, the kinematic viscosity is assumed to be constant, however experiments indicate that the assumption only

makes sense if temperature does not change rapidly for the application of interest. However, it has been noted that viscosity may change with temperature (see [21, 26, 34, 48, 50]), therefore, to predict more accurately the flow structure in industrial and engineering processes, it is necessary to consider this variation. Several temperature-dependent viscosity variation models have been presented in Table 1.1. Yürüsoy et al. [56] considered the flow of a third-grade fluid in a pipe with heat transfer. Constant viscosity, Reynolds' and Vogel's model viscosity cases are treated separately. Approximate analytical solutions are presented for each case using perturbation. Criteria for which the solutions are valid are determined for dimensionless parameters involved. Makinde [41] examined laminar falling liquid film with variable viscosity along an inclined plate. A steady flow is assumed and the coupled nonlinear equations were solved by the method of perturbation series summation and improvement technique. It was observed that an increase in the value of variable viscosity parameter signifies a decrease in fluid viscosity and an increase in value of Brinkman number. It was also noted that bifurcation point changes and tends to zero as the fluid viscosity decreases. Viscosity variation in a reactive flow also plays a very important role in the study of lava flows. Costa et al. [19, 20] examined viscous heating effects in fluids with temperature-dependent viscosity. They considered magma as incompressible and homogeneous fluid. They employed the Arrhenius type viscosity model but approximated it by (Nahme's or Reynold's) exponential law. They investigated the flow in an inclined slab between two parallel boundaries. They observed that viscous heating is responsible for increase of temperature near the walls with consequent local viscosity decrease. They also suggested the possibility of the formation of local flow instabilities at low Reynolds' number. In petrochemical industries and petroleum refineries, studies related to thermal ignition criticality and heat transfer in a reactive variable viscosity fluid are extremely useful. To this effect, Makinde [44] investigated the effect of Frank Kamenetskii and viscous heating parameter on thermal ignition of reactive fluids in a saturated porous medium. The Arrhenius type viscosity-temperature equation was employed. The governing equations were solved using regular perturbation methods improved with Hermite-Pade approximation techniques. It was observed that viscous heating enhances thermal ignition and steady flow of combustible fluid at low viscosity under Arrhenius kinetics ignites

faster than that at high viscosity. The fluid temperature increases with increasing values of viscous heating parameter. It was also observed that a combustible fluid at low viscosity flows faster than the one at high viscosity.

Furthermore, in a flow system, the hydrodynamic losses can be attributed to the frictional and local losses associated with the flow path changes. The hydrodynamic losses are irreversible and result in entropy generation in the flow system. Consequently, entropy generation gives insight into the amount of losses, which take place in the flow system. Entropy generation and minimization were investigated by Bejan [9, 10]. He showed the fundamental importance of entropy minimization for efficient processing. The second law analysis of combined heat and mass transfer in internal and external flows was considered by Carrington and Sun [15]. They introduced the entropy correlation, which could be used for internal and external flows. Heat transfer and entropy generation for a gravity-driven, non-Newtonian Ostwald–deWaele power-law, liquid film along an inclined isothermal plate was discussed by Makinde [42]. Entropy generation in a vertical concentric isothermal channel with temperature-dependent viscosity was considered by Tasnim and Mahmud [53]. They indicated that the maximum volumetric entropy generation is largely influenced by the fluid viscosity variation. The local entropy generation due to pressure gradient-assisted viscous flow between two parallel stationary plates when the plates are subjected to convective boundary conditions was investigated by Ibanez et al. [33]. They concluded that a minimum entropy generation rate can be achieved for certain combinations of the Biot number. Recently, Makinde [45, 46] investigated the effect of variable viscosity on thermodynamic irreversibility that occurs in plane Poiseuille flow with convective cooling at the walls. He reported that a decrease in fluid viscosity enhances the entropy-generation rate, while the dominant effect of heat transfer irreversibility near the channel walls decreases with an increase in convective cooling.

The present study sets out to investigate the inherent irreversibility in a reactive variable viscosity fluid flow in a channel under physically reasonable assumptions regarding the practical application in construction of engineering and industrial devices.

1.3 Problem Statement

In the industry, issues like productivity and competitiveness require engineering solutions which heavily relies on mathematical models. Therefore it is a major goal for the industry to understand the fluid behavior and heat transfer accurately in order to predict the flow regime of a reactive variable viscosity fluid. In order to have a clear understanding of the fluid dynamics in channel flow with two fixed parallel walls or with one wall fixed while the other wall is subjected to a uniform motion, it is very important to incorporate the heat transfer character of the fluid since this plays a very significant role in handling and processing of the material. In this project, a theoretical framework will be developed that would predict the nature of a reactive variable viscosity thin film flow with heat transfer in both an open and a closed channel.

1.4 Aim of the Study

This study aims to investigate theoretically the fluid dynamics of a reactive variable viscosity thin film flow and heat transfer in the channel flow system.

1.5 Objectives of the Study

To develop a mathematical model for a reactive variable viscosity thin film flow and heat transfer between (a) a fixed and a moving plate (b) two fixed parallel plates.
To determine the effects of various embedded parameters on both velocity and temperature profiles in the system.
To determine the effects of various embedded parameters on the entropy generation rate within the flow system. To provide a theoretical base for optimizing the efficiency of engineering devices and systems whose operation relies on a reactive variable viscosity channel flow.

CHAPTER

2

FLUID MECHANICS EQUATIONS

The following symbols are used in deriving fluid dynamics equations below:

ρ = fluid density
t = time
$\vec{q}$ = velocity vector
e = internal energy per unit mass
Φ = dissipation function
T = fluid temperature
p = fluid pressure
ν = kinematic viscosity
C_p = specific heat at constant pressure
k = thermal conductivity

2.1. CONTINUITY EQUATION

In a continuous fluid motion, if we consider a surface **S** fixed in space containing a volume **V**, it is clear that the increase in the mass of the fluid that flows in the system is the same as the mass of the fluid that flows out. The mass of the fluid within the system is

$$\int \rho dv. \qquad \textbf{(2.1.1)}$$

The rate of increase of the mass within the surface is given as

$$\frac{\partial}{\partial t}\int_v \rho dv = \int_v \frac{\partial \rho}{\partial t} dv \quad . \qquad \textbf{(2.1.2)}$$

Consider the following diagram and the fluid within the surface,

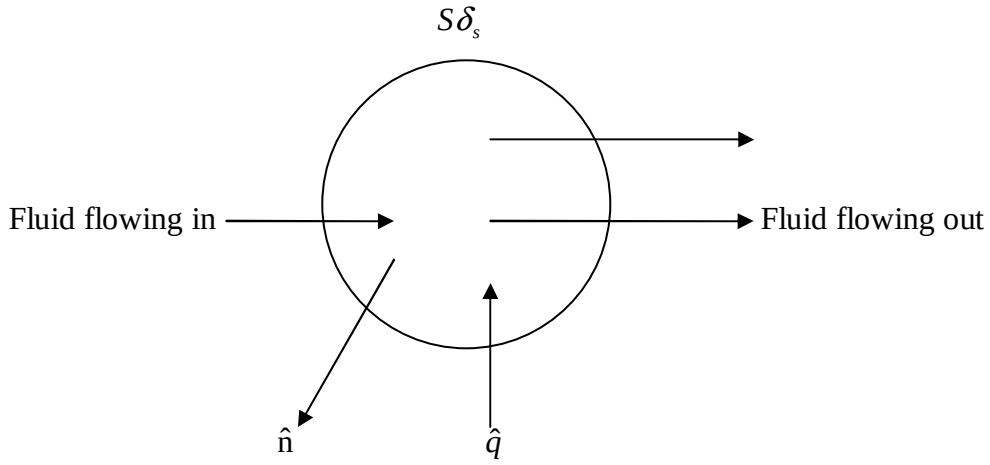

Fig. 2.1.1 Flow continuity diagram

Since **V** does not vary with time. The rate of flow through **S** is

$$\int_S (\vec{q}\cdot\vec{n})\rho ds = \int_v \nabla\cdot(\rho\vec{q})dv \qquad \textbf{(2.1.3)}$$

Thus

$$\int_v \frac{\partial \rho}{\partial t} dv = -\int_v \nabla\cdot(\rho\vec{q})dv \qquad \textbf{(2.1.4)}$$

$$\int_v \frac{\partial \rho}{\partial t} dv + \int_v \nabla \cdot (\rho \vec{q}) dv = 0 \qquad \textbf{(2.1.5)}$$

$$\int_v \left(\frac{\partial \rho}{\partial t} + div(\rho \vec{q}) \right) dv = 0 \qquad \textbf{(2.1.6)}$$

This is valid for any arbitrary volume V, the integral must identically vanish. Thus, we obtain

$$\frac{\partial \rho}{\partial t} + \text{div}(\rho \vec{q}) = 0 \qquad \textbf{(2.1.7)}$$

Equation **(2.1.7)** is called continuity equation for any fluid and it can be written as

$$\frac{\partial \rho}{\partial t} + \rho \text{div} \vec{q} + (\vec{q} \cdot \nabla) \rho = 0 \qquad \textbf{(2.1.8)}$$

i.e. $$\frac{D}{Dt} + \rho \text{div} \vec{q} = 0 \qquad \textbf{(2.1.9)}$$

where,

$$\frac{D}{Dt} = \frac{\partial}{\partial t} + \vec{q} \cdot \nabla$$

is the material derivative, which represents differentiation following fluid motion. For incompressible motion we have

$$\text{div} \vec{q} = 0 \qquad \textbf{(2.1.10)}$$

If

$$\vec{q} = (u, v, w)$$

then equation **(2.1.10)** reduces to

$$\frac{\partial u}{\partial x}+\frac{\partial v}{\partial y}+\frac{\partial w}{\partial z}=0 \qquad \textbf{(2.1.11)}$$

For 2D flow we usually write

$$\frac{\partial u}{\partial x}+\frac{\partial v}{\partial x}=0 \qquad \textbf{(2.1.12)}$$

In this case, we define the stream function ψ by:

$$u=\frac{\partial \psi}{\partial y} \text{ and } \quad v=-\frac{\partial \psi}{\partial x}$$

This equation satisfies the continuity equation:

$$u_x + u_y = (\psi_y)_x + (-\psi_x)_y = \psi_{yx} - \psi_{xy} \equiv 0$$

Now if the flow is irrotational then,

$$\nabla \times \vec{q} = 0$$

This implies that there exists a scalar function ϕ such that

$$\vec{q} = -\nabla \phi$$

In two dimensions we have

$$u=\frac{\partial \phi}{\partial x}, \quad v=-\frac{\partial \phi}{\partial y}$$

From **(2.1.12)**, we notice that ϕ satisfies Laplace's equations:

$$\frac{\partial^2 \phi}{\partial x^2} + \frac{\partial^2 \phi}{\partial y^2} = 0$$

2.2. LINEAR MOMENTUM EQUATION

Consider a small parallel piped of volume $dV = dx_1 \times dx_2 \times dx_3$, isolated instantaneous from the fluid element with center (x_1, x_2, x_3). We shall denote by σ_{ij} the stress acting in the x_i direction on the surface whose normal lies in the x_j direction. The stress component σ_{11}, σ_{12}, σ_{13}, etc., form a second order stress tensor σ_{ij}

i.e. $$\sigma_{ij} = \begin{bmatrix} \sigma_{11} & \sigma_{12} & \sigma_{13} \\ \sigma_{21} & \sigma_{22} & \sigma_{23} \\ \sigma_{31} & \sigma_{32} & \sigma_{33} \end{bmatrix} \qquad \textbf{(2.2.1)}$$

This is called the stress matrix. The components σ_{ii} are the normal stress while the components $\sigma_{ij(i \neq j)}$ are shear stresses. The stress tensor is symmetric. The corresponding stresses as the center of the face perpendicular to x_1:

$$\begin{aligned} &\sigma_{11} + \frac{1}{2}\frac{\partial \sigma_{11}}{\partial x_1} dx_{1,} \\ &\sigma_{12} + \frac{1}{2}\frac{\partial \sigma_{12}}{\partial x_1} dx_{1,} \\ &\sigma_{13} + \frac{1}{2}\frac{\partial \sigma_{13}}{\partial x_1} dx_{1,} \end{aligned} \qquad \textbf{(2.2.2)}$$

These are obtained from Taylor expansions of the form:

$$\sigma_{11}\left(dx_1, x_{2,} x_3\right) = \sigma_{11}(x_1, x_2, x_3) + \frac{1}{2}\frac{\partial \sigma_{11}}{\partial x_1} dx_1 + O(dx_1^2) \qquad \textbf{(2.2.3)}$$

At the centre of the opposite face, the corresponding stresses in the x_1 direction are:

$$\begin{aligned} &\sigma_{11} - \frac{1}{2}\frac{\partial \sigma_{11}}{\partial x_1} dx_{1,} \\ &\sigma_{12} - \frac{1}{2}\frac{\partial \sigma_{12}}{\partial x_1} dx_{1,} \\ &\sigma_{13} - \frac{1}{2}\frac{\partial \sigma_{13}}{\partial x_1} dx_{1,} \end{aligned} \qquad \textbf{(2.2.4)}$$

The stresses on a pair of opposite faces may be compounded into

$$\begin{aligned} &\frac{\partial \sigma_{11}}{\partial x_1} dx_1 dx_{2,} dx_{3,} \\ &\frac{\partial \sigma_{12}}{\partial x_2} dx_{1,} dx_{2,} dx_3, \\ &\frac{\partial \sigma_{13}}{\partial x_3} dx_{1,} dx_{2,} dx_3, \end{aligned} \qquad \textbf{(2.2.5)}$$

acting at parallel to $(0x_1, 0x_2, 0x_3)$. The stress on the other two pairs opposite forces may be compounded into similar forces at (x_1, x_2, x_3). The resultant force in x_1 the direction becomes

$$\left(\frac{\partial \sigma_{11}}{\partial x_1} + \frac{\partial \sigma_{21}}{\partial x_2} + \frac{\partial \sigma_{31}}{\partial x_3}\right) dx_1 dx_2 dx_3. \qquad \textbf{(2.2.6)}$$

If X, Y, Z are the forces per unit area due to variation of stress along $(0x_1, 0x_2, 0x_3)$, then

$$X = \frac{\partial \sigma_{11}}{\partial x_1} + \frac{\partial \sigma_{21}}{\partial x_2} + \frac{\partial \sigma_{31}}{\partial x_3} = \frac{\partial \sigma_{\alpha 3}}{\partial x_\alpha}$$

$$Y = \frac{\partial \sigma_{21}}{\partial x_1} + \frac{\partial \sigma_{22}}{\partial x_2} + \frac{\partial \sigma_{32}}{\partial x_3} = \frac{\partial \sigma_{\alpha 2}}{\partial x_\alpha} \qquad \textbf{(2.2.7)}$$

$$Z = \frac{\partial \sigma_{13}}{\partial x_1} + \frac{\partial \sigma_{23}}{\partial x_2} + \frac{\partial \sigma_{33}}{\partial x_3} = \frac{\partial \sigma_{\alpha 3}}{\partial x_\alpha}, \ \alpha = 1, 2, 3.$$

Generally we denote the body forces by **F** = $(F_1, F_2, F_3) = F_i, i = 1,2,3$**.** In this case, the equation of motion are:

$$\rho \frac{\partial U_i}{\partial t} = \frac{\partial \sigma_{ij}}{\partial x_J} + F_i \qquad \textbf{(2.2.8)}$$

In tensor notation we have $\vec{q} = (U_1, U_2, U_3) = U_i, i = 1,2,3$ i.e., the velocity vector. It is convenient to regard the stress σ_{ij} as the sum of inviscid part $-p\delta_{ij}$ and a viscous part σ_{ij} where *p* is the average of the three normal stresses for any orthogonal set of axes

$$p = \frac{\sigma_{ij}}{3}\delta_{ij} = \frac{1}{3}(\sigma_{11} + \sigma_{22} + \sigma_{33}) \qquad \textbf{(2.2.9)}$$

where δ_{ij} is the substitution tensor. Now separate the second tensor $\frac{\partial U_i}{\partial x_j}$ as follows,

$$\frac{\partial U_i}{\partial x_j} = \frac{1}{2}\left(\frac{\partial U_i}{\partial x_j} + \frac{\partial U_i}{\partial x_i}\right) + \frac{1}{2}\left(\frac{\partial U_i}{\partial xj} + \frac{\partial U_i}{\partial x_i}\right),$$

$$= \frac{1}{2}e_{ij} + \frac{1}{2}\gamma_{ij}. \qquad \textbf{(2.2.10)}$$

e_{ij} is the symmetric tensor while γ_{ij} is the anti-symmetric rotational tensor defining the velocity of the motion. In uniform media viscous stresses are induced only by deformation and not by rotation e_{ij} is called rate of strain tensor. It represents the rate of

change in the size and shape of a fluid element. The linear momentum equation now become

$$\rho\frac{d\vec{q}}{dt}=\rho\frac{\partial\vec{q}}{\partial t}+(\vec{q}\cdot\nabla)\vec{q}=-\nabla p+\nabla\cdot\sigma+\rho F \qquad \textbf{(2.2.11)}$$

In a Cartesian coordinate system, the second term on the r.h.s. of equation **(2.2.11)** is written:

$$\nabla\cdot\sigma=\left[\mu\left(\frac{\partial^2U_i}{\partial x_i\partial x_j}+\frac{\partial^2U_j}{\partial x_i^2}\right)+\frac{\partial\mu}{\partial x_i}\left(\frac{\partial U_i}{\partial x_j}+\frac{\partial U_j}{\partial x_i}\right)+\lambda\frac{\partial^2U_i}{\partial x_i\partial x_j}+\frac{\partial\lambda}{\partial x_j}\frac{\partial U_i}{\partial x_i}\right] \qquad \textbf{(2.2.12)}$$

Any additional simplification of $\nabla\cdot\sigma$ would require further assumptions or approximations.

2.3 ENERGY EQUATION

In order to derive the energy equation, we need to consider the zeroth and the first law of thermodynamics.

2.3.1 THE ZEROTH LAW OF THERMODYNAMICS

There exists the temperature T such that when two systems that are in contact are in thermal equilibrium, then T is the same in both systems. T is called the absolute temperature.

2.3.2 THE FIRST LAW OF THE THERMODYNAMICS

This expresses the principle of conservation of energy which states that there exists a variable of state, E, such that if a system is transformed from one state of equilibrium to another by the process in which an amount of work, W, is done on the system from the surrounding and the amount of heat, Q, is added to the system from the surroundings, then the difference between the initial and final values of energy of the systems E_i and E_f is given by

$$E_f - E_i = Q + W\,, \qquad \textbf{(2.3.2.1)}$$

In differential form we have

$$dE = dQ + dW\,, \qquad \textbf{(2.3.2.2)}$$

or

$$\frac{dE}{dt} = \frac{dQ}{dt} + \frac{dW}{dt}\,, \qquad \textbf{(2.3.2.3)}$$

In order to determine the work, we consider the first contribution from the component σ_{ij} of stress. The work in unit time is given by

$$\frac{\partial(W\sigma_{xx})}{\partial t} = dydz\left\{-U\sigma_{xx} + \left(U + \frac{\partial U}{\partial x}dx\right)\left(\sigma_{xx} + \frac{\partial \sigma_{xx}}{\partial x}dx\right)\right\} \qquad \textbf{(2.3.2.4)}$$

The total work done by the stress per unit mass on deforming elements of fluid is given by

$$\frac{1}{\rho}\frac{\partial(\sigma_{ij}U_j)}{\partial x_i} = \frac{1}{2}\left(\frac{\partial \sigma_{ij}}{\partial x_i} + \sigma_{ij}\frac{\partial U_j}{\partial x_i}\right), \qquad \textbf{(2.3.2.6)}$$

Where σ_{ij} is the stress acting in the x_i on the face whose normal lies in the x_j direction. From the equation of fluid motion, we have

$$\rho \frac{\partial U_i}{\partial t} = \frac{\partial (\sigma_{ij})}{\partial x_i} \qquad \textbf{(2.3.2.7)}$$

and hence

$$U_j \frac{\partial (\sigma_{ij})}{\partial x_i} = \rho U_i \frac{\partial U_i}{\partial t} = \frac{\rho}{2} \frac{d(U_i U_j)}{dt} \qquad \textbf{(2.3.2.8)}$$

This is clearly the change in kinematic energy of the fluid element following motion. The remaining term in equation **(2.1.3.2.8)** represents the rate of dissipation of energy per unit mass. Substituting $\sigma_{ij} = -p\delta_{ij} + \mu e_{ij}$

$$\frac{\partial W}{\partial t} = \frac{1}{2} \frac{\partial (U_i U_j)}{\partial t} - \frac{p}{\rho} \sigma_{ij} \frac{\partial U_j}{\partial x_i} + \upsilon \frac{\partial U_i}{\partial x_i} \left(\frac{\partial U_i}{\partial x_i} + \frac{\partial U_j}{\partial x_i} \right) \qquad \textbf{(2.3.2.9)}$$

But

$$\delta_{ij} \frac{\partial U_j}{\partial x_i} = \frac{\partial U_i}{\partial x_i} = 0$$

It is clear that only viscous forces and not pressure forces contribute to energy dissipation. Define the energy dissipation function Φ by

$$\Phi = \frac{\partial \mathrm{U_j}}{\partial \mathrm{x_i}} \left(\frac{\partial \mathrm{U_i}}{\partial \mathrm{x_i}} + \frac{\partial \mathrm{U_j}}{\partial \mathrm{x_i}} \right) = \frac{1}{2} \left(\frac{\partial U_i}{\partial x_i} + \frac{\partial U_j}{\partial x_i} \right)^2 \qquad \textbf{(2.3.2.10)}$$

Showing that $\Phi \geq 0$ and we have,

$$\frac{dW}{dt} = \frac{1}{2} \frac{d}{dt} (U_i U_j) + \upsilon \Phi \qquad \textbf{(2.3.2.11)}$$

Similarly the heat transferred to the system from the surrounding is Q. We shall neglect the transfer of heat by radiation and consider only that by conduction. If we consider the element of the volume, $dV = dxdydz$ of the mass ρdv and the change in kinetic energy of an amount

$$d\left\{\frac{1}{2}\rho dv(U_1^2+U_2^2+U_3^2)\right\}, \qquad \textbf{(2.3.2.12)}$$

and neglecting change in potential energy, we then have

$$\frac{dE}{dt}=\rho dV\left\{\frac{de}{dt}+\frac{1}{2}\frac{d(U_1^2+U_2^2+U_3^2)}{dt}\right\}, \qquad \textbf{(2.3.2.13)}$$

where e is the thermal energy per unit mass.

2.3.3 FOURIER CONDUCTION

This law states that the heat flux **q** per unit area and time is proportional to the temperature gradient, i.e.,

$$\mathbf{q}=\frac{1}{A}\frac{\partial Q}{\partial t}=-k\frac{\partial T}{\partial n} \qquad \textbf{(2.3.3.1)}$$

or,

$$\mathbf{q}-k\nabla T$$

where k is the thermal conductivity. The negative sign signifies that the heat flux is reckoned as positive in the direction of temperature gradient (i.e. heat flux is in the direction of decreasing temperature). Hence the amount of heat transferred into the volume dV through surface elements which are normal to the x direction is equal

$$\left(-k\frac{\partial T}{\partial n}\right)dydz, \qquad \textbf{(2.3.3.2)}$$

The amount of heat leaving the volume is given by

$$\left[k\frac{\partial T}{\partial x} + \frac{\partial}{\partial x}\left(k\frac{\partial T}{\partial x} \right) dx \right] dydz\,, \qquad \textbf{(2.3.3.3)}$$

Thus the amount of heat added by conduction in the direction during time *dt* to volume *dV* is

$$dt \cdot dV \frac{\partial}{\partial x}\left(k\frac{\partial T}{\partial x} \right)$$

Hence, the total amount of heat added in all directions is given by

$$\frac{\partial Q}{\partial t} = dV\left[\frac{\partial}{\partial x}\left(k\frac{\partial T}{\partial x} \right) + \frac{\partial}{\partial y}\left(k\frac{\partial T}{\partial y} \right) + \frac{\partial}{\partial z}\left(k\frac{\partial T}{\partial z} \right) \right] \qquad \textbf{(2.3.3.4)}$$

Using equations **(2.3.2.13)** and **(2.3.3.4)** we obtain

$$\rho\frac{\partial e}{\partial t} = \frac{\partial}{\partial x}\left(k\frac{\partial T}{\partial x} \right) + \frac{\partial}{\partial y}\left(k\frac{\partial T}{\partial y} \right) + \frac{\partial}{\partial z}\left(k\frac{\partial T}{\partial z} \right) + \upsilon\Phi \qquad \textbf{(2.3.3.5)}$$

where,

$$\Phi = 2\left\{ \left(\frac{\partial U_1}{\partial x} \right)^2 + \left(\frac{\partial U_2}{\partial y} \right)^2 + \left(\frac{\partial U_3}{\partial z} \right)^2 \right\} + \left(\frac{\partial U_1}{\partial y} + \frac{\partial U_2}{\partial x} \right)^2 + \left(\frac{\partial U_3}{\partial y} + \frac{\partial U_2}{\partial z} \right)^2 + \left(\frac{\partial U_1}{\partial z} + \frac{\partial U_3}{\partial x} \right)^2$$

Equation **(2.3.3.5)** holds for an incompressible fluid with constant thermal conductivity *k*. For perfect fluid,

$$\frac{de}{dt} = C_v\frac{dT}{dt}, (de = C_v dT) \qquad \textbf{(2.3.3.6)}$$

Equation **(2.3.3.5)** now takes the form

$$\rho C_v \frac{dT}{dt} = k\nabla^2 T + \mu\Phi \qquad \textbf{(2.3.3.7)}$$

This is the energy equation where C_v is the specific heat at constant volume. Equation **(2.3.3.7)** can be written as

$$\rho C_v \left(\frac{\partial T}{\partial t} + (\vec{q} \cdot \nabla) T \right) = k\nabla^2 T + \mu\Phi \qquad \textbf{(2.3.3.8)}$$

Where Φ is small relative to $\rho C_v \frac{dT}{dt}$, equation **(2.3.3.7)** becomes

$$\frac{\partial T}{\partial t} = \frac{k}{\rho C_v} \nabla^2 T = \frac{\nu}{\sigma} \nabla^2 T \,, \qquad \textbf{(2.3.3.9)}$$

where

$\sigma = \frac{\mu C_v}{k}$ is the Prandtl number

In rectangular coordinates, equation **(2.3.3.9)** reads:

$$\frac{\partial T}{\partial t} + U_1 \frac{\partial T}{\partial x} + U_2 \frac{\partial T}{\partial y} + U_3 \frac{\partial T}{\partial z} = \frac{\upsilon}{\sigma} \left(\frac{\partial^2 T}{\partial x^2} + \frac{\partial^2 T}{\partial y^2} + \frac{\partial^2 T}{\partial z^2} \right) \qquad \textbf{(2.3.3.10)}$$

2.4. GENERAL FORM OF THE SECOND LAW THERMODYNAMICS.

The first part of the second law postulates a thermodynamic state variable, the entropy, defined by

$$(d\tilde{q})_{rev} = Tds$$

as

$$ds = \frac{(d\tilde{q})_{rev}}{T} \qquad \textbf{(2.4.1)}$$

This definition was originally for a simple, closed system, where $(d\tilde{q})_{rev}$ is the reversible heat transfer that crosses the system's boundary and T is the absolute temperature of the surrounding medium at the boundary. Form this definition and the first law of thermodynamics, the relation for a closed system

$$Tds = dh - \frac{dp}{\rho}$$

is obtained. This equation can be extended to an open system by writing it as

$$Tds = dh - \frac{dp}{\rho} - \sum_{\alpha} \tilde{\mu}_{\alpha} dy_{\alpha} \qquad \textbf{(2.4.2)}$$

If *h* and *p* are held constant, then $-\mu_{\alpha}/T$ provides the entropy change associated with the unit compositional change dy_{α} in species α. Thus, the chemical potential enables us to consider mass transfer across the boundary as well as compositional changes within the system. This extension is essential if chemical reactions, phase changes, or diffusion are present. Moreover, the heat transfer in equation **(2.4.1)** is now not restricted to conduction

but may encompass any reversible heat transfer process including mass diffusion, chemical reactions, and the transport of radiative energy.

2.5 DERIVATION OF THE PRODUCTION OF ENTROPY

For the thermodynamic system, we utilize an infinitesimal fluid particle that moves with velocity U but may have diffusional fluxes at its boundary. In this circumstance, we can r]

eplace the thermodynamic derivatives in equation **(2.4.2)** with the substantial derivative to obtain

$$T\frac{Ds}{Dt}=\frac{Dh}{Dt}-\frac{1}{\rho}\frac{Dp}{Dt}-\sum_{\alpha}\tilde{\mu}_{\alpha}\frac{Dy_{\alpha}}{Dt} \qquad \textbf{(2.5.1)}$$

We now use the general form of the energy equation, i.e

$$\rho\frac{D\bar{h}}{Dt}=\frac{D\bar{p}}{Dt}-\nabla\cdot\vec{q}+\Phi\,, \qquad \textbf{(2.5.2)}$$

without the over bars, to eliminate Dh/Dt and the following relation

$$\rho\frac{Dy_{\alpha}}{Dt}=\rho\dot{\omega}_{\alpha}-\nabla\cdot\vec{j}_{\alpha},\alpha=1,...,N \qquad \textbf{(2.5.3)}$$

to eliminate Dy_{α}/Dt, with the results

$$T\frac{Ds}{Dt}=\frac{1}{\rho}\left(\frac{Dp}{Dt}-\nabla\cdot\vec{q}+\Phi\right)-\frac{1}{\rho}\frac{Dp}{Dt}-\sum_{\alpha}\tilde{\mu}_{\alpha}(\dot{\omega}_{\alpha}-\frac{1}{\rho}\nabla\cdot\vec{j}_{\alpha})$$

or

$$\rho\frac{Ds}{Dt}=\frac{1}{T}\left(\Phi-\rho\sum_{\alpha}\tilde{\mu}_{\alpha}\dot{\omega}_{\alpha}-\nabla\cdot\vec{q}+\sum\tilde{\mu}_{\alpha}\nabla\cdot\vec{j}_{\alpha}\right)$$

This relation provides the rate of change of entropy of a fluid particle, where part of this change is due to the transport of entropy of a fluid across the system's boundary, as given by $(d\tilde{q})_{rev}/T$. In order to focus on entropy transport, in contrast to energy transport, we replace $\vec{q}$ by $\vec{q}^{*}$. This alteration is conveniently accomplished by the rightmost two terms in the above equation as

$$-\nabla\cdot\vec{q}+\sum_{\alpha}\tilde{\mu}_{\alpha}\nabla\cdot\vec{j}_{\alpha}=-\nabla\cdot\left(\vec{q}^{*}+\sum_{\alpha}\tilde{\mu}_{\alpha}\vec{j}_{\alpha}\right)+\sum_{\alpha}\vec{j}_{\alpha}\cdot\nabla\tilde{\mu}_{\alpha}$$

$$=-\nabla\cdot\vec{q}^{*}-\sum_{\alpha}\vec{j}_{\alpha}\cdot\nabla\tilde{\mu}_{\alpha}-\sum_{\alpha}\tilde{\mu}_{\alpha}\nabla\cdot\vec{j}_{\alpha}+\sum_{\alpha}\tilde{\mu}_{\alpha}\nabla\cdot\vec{j}_{\alpha}$$

$$=-\nabla\cdot\vec{q}^{*}-\sum_{\alpha}\vec{j}_{\alpha}\cdot\tilde{\mu}_{\alpha}\nabla \qquad \textbf{(2.5.4)}$$

to obtain

$$\rho\frac{Ds}{Dt}=\frac{1}{T}\left[\Phi-\sum_{\alpha}(\rho\tilde{\mu}_{\alpha}\dot{\omega}_{\alpha}+\vec{j}_{\alpha}\cdot\nabla\tilde{\mu}_{\alpha})\right]-\frac{1}{T}\nabla\cdot\vec{q}* \qquad \textbf{(2.5.5)}$$

In equation **(2.4.1)**, the temperature is that of the surface of the system. In $\nabla\cdot\vec{q}^{*}/T$, the temperature is that of the interior of the fluid particle; hence, this term is *not* the counterpart of $(d\tilde{q})_{rev}^{*}/T$. We observe that the quantity we seek is provided by the surface integral

$$\int_{\delta s} \hat{n} \cdot \left(\frac{\vec{q}^*}{T} \right) ds$$

where δs is the surface area of a fluid particle. By using the following equation

$$\nabla \cdot \vec{A} = \lim_{\delta v \to 0} \frac{1}{\delta v} \int \hat{n} \cdot \vec{A} ds \qquad \textbf{(2.5.6)}$$

we have

$$\nabla \cdot \left(\frac{\vec{q}^*}{T} \right) = \lim_{\delta v \to 0} \frac{1}{\delta v} \int_{\delta s} \hat{n} \left(\frac{\vec{q}^*}{T} \right) ds \qquad \textbf{(2.5.7)}$$

Thus, $\nabla \cdot (\vec{q}^* / T)$ corresponds to the entropy transport into or out of the particle. From the definition of $\vec{q}^*$, i.e., the following equation

$$\vec{q}^* = -\kappa \nabla T + \sum_{\alpha} (h_\alpha - \tilde{\mu}_\alpha) \vec{j}_\alpha + \vec{q}_R \,, \qquad \textbf{(2.5.8)}$$

we observe that the heat conduction, mass transfer, and radiative heat transfer contribute to the entropy transport, but that viscous effects and chemical reactions do not. As observed in the previous section, the mass transfer contribution is associated with entropy flux

$$\frac{1}{T} \sum (h_\alpha - \tilde{\mu}_\alpha) \vec{j}_\alpha = \sum_{\alpha} s_\alpha \vec{j}_\alpha \qquad \textbf{(2.5.9)}$$

when $\tilde{\mu}_\alpha$ is replace by

$$\tilde{\mu}_\alpha = h_\alpha - T s_\alpha \qquad \textbf{(2.5.10)}$$

We introduce $\nabla \cdot (\vec{q}^{*}/T)$ into equation **(2.5.5)** by means of the identity

$$\nabla \cdot \left(\frac{\vec{q}^{*}}{T} \right) = \frac{1}{T} \nabla \cdot \vec{q}^{*} + \vec{q}^{*} . \nabla \frac{1}{T} = \frac{1}{T} \nabla \cdot \vec{q}^{*} - \frac{1}{T^{2}} \vec{q}^{*} \cdot \nabla T$$

to obtain

$$-\frac{1}{T} \nabla \cdot \vec{q}^{*} = -\nabla \cdot \frac{\vec{q}^{*}}{T} - \frac{1}{T^{2}} \vec{q}^{*} \cdot \nabla T \qquad \textbf{(2.5.11)}$$

With these relations, equation **(2.5.5)** becomes

$$\rho \frac{Ds}{Dt} = \rho \dot{s}_{irr} - \nabla \cdot \frac{\vec{q}^{*}}{T} \qquad \textbf{(2.5.12)}$$

where the rate of entropy production, per unit volume of the mixture, is given by

$$\rho \dot{s}_{irr} \frac{1}{T} \left[\Phi - \frac{1}{T} \vec{q}^{*} \cdot \nabla T - \sum_{\alpha} \rho \tilde{\mu}_{\alpha} \dot{\omega}_{\alpha} + \vec{j}_{\alpha} \cdot \nabla \tilde{\mu}_{\alpha} \right] \qquad \textbf{(2.5.13)}$$

Our presentation of the first part of the second law, which started with Equation **(2.4.1)**, has culminated in Equations **(2.5.12)** and **(2.5.13)**. The second part of the law states that

$$\dot{s}_{irr} = 0 \qquad \textbf{(2.5.14)}$$

for a reversible process and

$$\dot{s}_{irr} > 0 \qquad \textbf{(2.5.15)}$$

for an irreversible process. Although $\dot{s}_{irr}$ is nonnegative, Ds/Dt can be negative, since the divergence term in Equation **(2.5.12)** can have either sign.

2.6. DISCUSSION

The rate of entropy production, $\dot{s}_{irr}$, represents the irreversible processes that occur within a fluid particle. Hence, the entropy changes due to internal processes and entropy transport into or out of the particle. With the assistance of the methods discussed in *transport theorem,* Equation **(2.5.12)** can be written as

$$\frac{D}{Dt}\int_V \rho s dv = \int_V \rho \dot{s}_{irr} dv - \int_S \tilde{n}\left(\frac{\vec{q}^*}{T}\right) ds \qquad \textbf{(2.6.1)}$$

By way of illustration, consider a mixture of thermally perfect gases that are diffusionally mixing. With this as the only process we have

$$\vec{q}^* = \sum_\alpha (h_\alpha - \tilde{\mu}_\alpha)\vec{j}_\alpha = T\sum_\alpha s_\alpha \vec{j}_\alpha \qquad \textbf{(2.6.2)}$$

or

$$\frac{\vec{q}^*}{T} = \sum_\alpha s_\alpha \vec{j}_\alpha \qquad \textbf{(2.6.3)}$$

where Equation **(2.1.5.10)** is utilized. Consequently the $\hat{n}\cdot\vec{j}_\alpha$ appearing in the rightmost term in Equation **(2.1.5.13)** now reduces to

$$\frac{1}{T}\left(-\frac{1}{T}\vec{q}^*\cdot\nabla T - \sum_\alpha \vec{j}_\alpha\cdot\nabla\tilde{\mu}_\alpha\right) = -\frac{1}{T}\left[\sum_\alpha s_\alpha\vec{j}_\alpha\cdot\nabla T + \sum_\alpha \vec{j}_\alpha\cdot\nabla(h_\alpha - Ts_\alpha)\right]$$

$$= \sum_\alpha \vec{j}_\alpha\cdot\left(\nabla s_\alpha - \frac{1}{T}\nabla h_\alpha\right) \qquad \textbf{(2.6.4)}$$

Thus, a dot product involving $\vec{j}_\alpha$ appears in each of the terms on the right-hand side of Equation **(2.6.4)**. The first of these, however, is internal to the system, whose volume is V, whereas the second one is evaluated on the boundary of the system.

Viscous effects and chemical reactions enter through Φ and $\dot{\omega}_\alpha$, respectively, and are internal processes that appear only in $\dot{s}_{irr}$. Evidently, the contribution of viscous dissipation to $\dot{s}_{irr}$ is zero when both μ and μ_b are zero or when the velocity gradient is zero. The contribution from reactions is zero when the flow is chemically frozen, i.e., all $\dot{\omega}_\alpha$ are zero or when the reactions are in equilibrium, in which case the sum $\sum \tilde{\mu}_\alpha \dot{\omega}_\alpha$ is zero. Conduction heat transfer, radiative heat transfer, and mass diffusion, through $\vec{q}^*$, appear in both $\dot{s}_{irr}$ and in $\nabla \cdot (\vec{q}^*/T)$. The analysis has not ruled out body forces or restricted the acceleration, DU/Dt, in any manner. A purely accelerative inviscid flow or the work due to a body force does not result in any (irreversible) production of entropy.

2.7. HEAT TRANSFER

Because $\vec{q}$ is *not* a state variable, we write $d\tilde{q}_{rev}/dt$ as $\dot{\tilde{q}}_{rev}$ rather than as $D\tilde{q}_{rev}/Dt$ when following a fluid particle. Thus, Equation **(2.4.1)** can be written as

$$T\frac{Ds}{Dt} = \dot{\tilde{q}}_{rev} \qquad \textbf{(2.7.1)}$$

and $T(Ds/dt)$ represents the amount of heat gained, per unit time and per unit mass, by a fluid particle undergoing a reversible process. By comparing this result with Equation **(2.5.12)** we have

$$\dot{\tilde{q}}_{rev} = -\frac{T}{\rho}\nabla \cdot \frac{\vec{q}^*}{T} \qquad \textbf{(2.7.2)}$$

for a reversible process, where $\dot{s}_{irr} = 0$. This relation is not equivalent to

$$\bar{d}\vec{q} = -\nu(\nabla \cdot \vec{q})dt\,, \qquad \textbf{(2.7.3)}$$

which holds for an irreversible or reversible process of a closed, simple system.

For a general process, $T(Ds/Dt)$ still represents the heat transfer to a fluid particle. We see from Equation **(2.5.12)** that the heat gained is due to $\dot{s}_{irr}$ and $\vec{q}^{*}$.it is tempting to partition the heat transfer between reversible and irreversible contributions, as was done with the work. i.e.,

$$\bar{d}W = -\rho dv + \nu\Phi dt \qquad \textbf{(2.7.4)}$$

Such decomposition however is not justified, as can be seen from the following argument. Consider a process consisting solely of irreversible conductive heat transfer. In this case, we have

$$\vec{q}^{*} = \vec{q} = -\kappa\nabla T$$

which appears in both the $\dot{s}_{irr}$ term and the divergence term on the right side of Equation **(2.5.12)**. Appearing, as it does, in both terms, the heat transfer $\vec{q}$ cannot be split into both a reversible and irreversible component.

2.8. SECOND LAW FOR A VISCOUS, HEAT CONDUCTING FLOW

We suppose that only viscous stresses and conductive heat transfer are present. In this circumstance, Equations **(2.5.12)** and **(2.5.13)** become

$$\rho\frac{Ds}{Dt} = \rho\dot{s}_{irr} - \nabla \cdot \frac{\vec{q}}{T} \qquad \textbf{(2.8.1)}$$

$$\rho \dot{s}_{irr} = \frac{1}{T}\left(\Phi - \frac{1}{T}\vec{q} \cdot \nabla T \right) \qquad \textbf{(2.8.2)}$$

where $\vec{q}$ is now the conductive heat flux. If we further assume Fourier's equation and a Newtonian fluid, we have

$$\rho \frac{Ds}{Dt} = \rho \dot{s}_{irr} + \nabla \cdot \left(\frac{\kappa}{T} \nabla T \right) \qquad \textbf{(2.8.3)}$$

$$\rho \dot{s}_{irr} = \frac{1}{T}\left[\Phi + \frac{\kappa}{T} (\nabla T)^2 \right] \qquad \textbf{(2.8.4)}$$

Where Φ is provided by the following Equations

$$\Phi = 2\mu \in_{ij} \in_{ii} + 4\mu(\in_{12}^2 + \in_{23}^2 + \in_{31}^2) + \lambda(\in_{ii})^2 \qquad \textbf{(2.8.4.1)}$$

or

$$\Phi = \mu \left[2\sum_{i=1}^{3} \left(\frac{\partial U_i}{\partial x_i} \right)^2 + \left(\frac{\partial U_1}{\partial x_2} + \frac{\partial U_2}{\partial x_1} \right)^2 + \left(\frac{\partial U_2}{\partial x_3} + \frac{\partial U_3}{\partial x_2} \right)^2 + \left(\frac{\partial U_3}{\partial x_1} + \frac{\partial U_1}{\partial x_3} \right)^2 \right] + \lambda \left(\sum_{i=1}^{3} \frac{\partial U_i}{\partial x_i} \right)^2$$

(2.8.4.2).

The second law requires $\dot{s}_{irr} \geq 0$ for any realizable process. By detailed balancing, this must hold individually for the heat transfer and the viscous work. We, therefore, require

$$\kappa \geq 0, \qquad \Phi \geq 0 \qquad \textbf{(2.8.5)}$$

For heat conduction, the second law is satisfied providing the coefficient of thermal conductivity is nonnegative.

From Equation **(2.8.4.2)**, it would appear that the $\Phi \geq 0$ condition is satisfied if μ and λ are nonnegative. While μ is nonnegative, λ may be negative as is evident from Stokes' hypothesis, which presumes $\lambda = -(2\mu/3)$.

To determine the minimum allowed value for λ, we consider a purely dilatational motion in which case a is a constant. In such a flow all shearing stress terms are zero. For this flow, Equation **(2.8.4.2)** readily yields

$$\Phi = \mu\left[2(3a^2)\right] + \lambda(3a)^2 = 9\left(\lambda + \frac{2}{3}\mu\right)a^2 = 9\mu_b a^2 \qquad \textbf{(2.8.6)}$$

where μ_b is the bulk viscosity. However any constraint on μ, λ, or κ, must be independent of the assumed flow model, since these parameters are material properties. A necessary condition, therefore, for $\Phi \geq 0$ is that $\mu_b \geq 0$.

Observe from Equation **(2.8.4.2)** that the shearing velocity derivatives only occur in the μ part of Φ and then always in squared terms. Hence, the μ term is the minimum when these shearing derivatives are zero and Φ is similarly minimized. This only leaves the dilatation terms, which are dealt with in the above paragraph. Thus, $\mu \geq 0$ and $\mu_b \geq 0$ are the necessary and sufficient conditions for $\Phi \geq 0$. In turn, we see that the second law simply requires

$$\kappa \geq 0 \qquad \mu \geq 0 \qquad \mu_b \geq 0 \qquad \textbf{(2.8.6)}$$

for a flow where Fourier's equation and a Newtonian fluid are utilized. When this other terms are negligible, as is often the case in fluid dynamics, thus we have

$$\dot{s}_{irr} = 0, \qquad \frac{Ds}{Dt} = 0 \qquad \textbf{(2.8.7)}$$

In summary the basic fluid dynamics equations needed for our studies are outlined below. (see, Batchelor,(1991)).

2.9. General Form for:

I. CONTINUITY EQUATION

$$\frac{\partial \rho}{\partial t} + \vec{q} \cdot \nabla \rho = 0$$

II. LINEAR MOMENTUM EQUATION

$$\nabla \cdot \vec{\sigma} = \left[\mu \left(\frac{\partial^2 U_i}{\partial x_i \partial x_j} + \frac{\partial^2 U_j}{\partial x_i^2} \right) + \frac{\partial \mu}{\partial x_i} \left(\frac{\partial U_i}{\partial x_j} + \frac{\partial U_j}{\partial x_i} \right) + \lambda \frac{\partial^2 U_i}{\partial x_i \partial x_j} + \frac{\partial \lambda}{\partial x_j} \frac{\partial U_i}{\partial x_i} \right]$$

III. ENERGY EQUATION

$$\frac{dT}{dt} = \frac{\partial T}{\partial t} + (\vec{q} \bullet \nabla) T = \frac{\upsilon}{\sigma} \nabla^2 T + \frac{\upsilon}{C_v} \Phi$$

where

$$\sigma = \frac{\mu C_v}{k}$$

IV. ENTROPY GENERATION EQUATION

$$\rho \dot{s}_{irr} = \frac{1}{T} \left[\Phi + \frac{\kappa}{T} (\nabla T)^2 \right]$$

CHAPTER

3

ENTROPY ANALYSIS FOR VARIABLE VISCOSITY REACTIVE COUETTE FLOW

3.1. Introduction

In fluid dynamics, Couette flow refers to the laminar flow of a viscous fluid in the space between two parallel plates, one of which is moving relative to the other. This type of flow is named in honor of Maurice Marie Alfred Couette, a Professor of Physics at the French university of Angers in the late 19th century [8, 60]. Couette flow occurs in fluid machinery involving moving parts and is especially important for hydrodynamic lubrication [62]. If the surfaces are smooth and flat with constant fluid properties, the solution is the simple linear velocity distribution, with a drag proportional to the relative velocity and inversely proportional to the gap width [6, 8]. It is an important classical example of exact solutions for Navier-Stokes equation. However, most fluids used in engineering and industrial systems like coal slurries, polymer solutions or melts, drilling mud, hydrocarbon oils, grease, etc., are chemically reactive and can be subjected to extreme conditions, such as high temperature, pressure and shear rate during processing [34, 61]. In fact, viscous heating produced due to friction between the fluid and the surrounding walls coupled with high shear rates and Arrhenius kinetics can lead to high temperatures being generated within the fluid [78]. This may have a significant effect on the fluid properties. It is well known that the most sensitive fluid property to temperature rise is the viscosity [34, 62]. For instance, the viscosity of various lubricants used in engineering systems like polymer solutions, mineral oils

with polymeric additives, etc., varies with temperature. This variation in the fluid viscosity due to temperature may affect the flow characteristics as well as the efficient operation of industrial machinery where lubrication is important [8, 78]. Hence, it is necessary to ensure that the viscosity of such lubricants is at all times maintained at optimum levels.

From the application point of view, the determination of thermal criticality in a flow system is extremely important. For example, special attention must be paid to the heating of lubricant by the frictional force and Arrhenius kinetics since viscosity is temperature dependent. Thermal criticality occurs when the rate of heat generation within the flow system exceeds the heat dissipation to the surroundings [60, 61]. This condition is incipient thermal runaway or ignition in the flow system [45, 78]. A primary objective of thermal criticality analysis is the prediction of the critical or unsafe flow conditions in order to avoid them [58]. One method of accomplishing this is to cycle the lubricant through a cooling reservoir in order to maintain the desired viscosity of the fluid. Another way of handling the excessive heat generation problem is to use commercially available additives to decrease the viscosity's temperature dependence.

Meanwhile, thermodynamic irreversibility occurs in the flow system due to fluid friction and heat transfer. The amount of thermodynamic irreversibility gives insight into the losses associated within the thermal system. Entropy production rate provides information on the amount of thermodynamic irreversibility in the system. Consequently, prediction of entropy generation due to different flow conditions enables one to determine the flow system with minimized losses. In his pioneering work, Bejan [8, 9] reported the fundamental importance of entropy generation and minimization in engineering systems. Thereafter, considerable research works were carried out by several authors on the application of second law of thermodynamics to various aspects of fluid flow and heat transfer problems [6, 7, 9, 10, 15, 33, 42, 43, 53]. Moreover, to the best of our knowledge, no study has focused on the combined effects of temperature dependent fluid viscosity and Arrhenius kinetics on thermal stability and entropy generation and minimisation in a flow system.

In this study, the variable viscosity reactive Couette flow is considered and the inherent irreversibility together with thermal criticality in the flow system is investigated. The plan of this chapter is as follows; in section two we describe the theoretical analysis of the problem with respect to the fluid velocity and temperature fields. In sections three to five we introduce and apply some rudiments of perturbation techniques coupled with Hermite-Padé approximation procedures and standard Newton–Raphson shooting method along with a fourth-order Runge–Kutta integration algorithm in order to obtain the fluid velocity temperature profiles as well as criticality conditions in the system. Section six describes the volumetric entropy generation rate, irreversibility distribution ratio and the Bejan number. The results are presented graphically and discussed quantitatively in section seven.

3.2. Problem Formulation

The configuration of the problem studied in this paper is depicted in **Fig. 3.2.1.** The fluid is assumed to be viscous, incompressible, reactive and flowing steadily in the $\bar{x}$-direction between two parallel plates of width *H* and length *L*. The upper plate is moving with constant velocity *U* while the lower plate is kept stationary. Following [45, 62] the temperature dependent viscosity ($\bar{\mu}$) and the chemical reaction kinetic (*G*) functions can be expressed in Arrhenius type [59] as

$$\bar{\mu} = \mu_0 e^{\frac{E}{R\bar{T}}}, \quad G = QC_0 Ae^{-\frac{E}{R\bar{T}}} \tag{3.2.1}$$

where *E* is the activation energy, *R* is the universal gas constant, *Q* is the heat of reaction, *A* is the rate constant, C_0 is the initial concentration of the reactant species and μ_0 is the fluid reference dynamic viscosity at a very large temperature (i.e. as $\bar{T} \to \infty$).

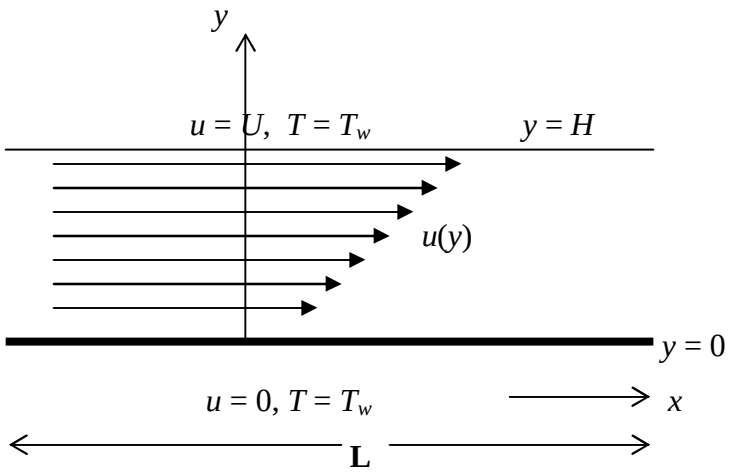

Figure 3.2.1: Schematic diagram of the problem.

Under these conditions the continuity, momentum and energy equations governing the problem in dimensionless form may be written as [8, 34, 60];

$$\frac{\partial u}{\partial x}+\frac{\partial v}{\partial y}=0, \qquad \textbf{(3.2.2)}$$

$$Re\left(u\frac{\partial u}{\partial x}+v\frac{\partial u}{dy}\right)=-\frac{\partial p}{\partial x}+2\varepsilon^2\frac{\partial}{\partial x}\left(\mu\frac{\partial u}{\partial x}\right)+\frac{\partial}{\partial y}\left[\mu\left(\frac{\partial u}{\partial y}+\varepsilon^2\frac{\partial v}{\partial x}\right)\right], \qquad \textbf{(3.2.3)}$$

$$Re\left(u\frac{\partial v}{\partial x}+v\frac{\partial v}{\partial y}\right)=-\frac{\partial p}{\partial y}+2\varepsilon^2\frac{\partial}{\partial y}\left(\mu\frac{\partial v}{\partial y}\right)+\varepsilon^2\frac{\partial}{\partial x}\left[\mu\left(\frac{\partial u}{\partial y}+\varepsilon^2\frac{\partial v}{\partial x}\right)\right], \qquad \textbf{(3.2.4)}$$

$$\varepsilon^2 Pe\left(u\frac{\partial T}{\partial x}+v\frac{\partial T}{\partial y}\right)=\varepsilon^2\frac{\partial^2 T}{\partial x^2}+\frac{\partial^2 T}{\partial y^2}+\lambda e^{\left(\frac{T}{1+\beta T}\right)}+\mu\Phi, \qquad \textbf{(3.2.5)}$$

where

$$\Phi = \mathrm{Br}\left[2\varepsilon^2\left(\frac{\partial u}{\partial x}\right)^2 + 2\varepsilon^2\left(\frac{\partial v}{\partial y}\right)^2 + \left(\frac{\partial u}{\partial y} + \varepsilon^2\frac{\partial v}{\partial x}\right)^2\right]. \qquad \textbf{(3.2.6)}$$

We have employed the following non-dimensional quantities in Eqs. **(3.2.2)- (3.2.6)**:

$$\left\{\begin{array}{l} y = \dfrac{\overline{y}}{\varepsilon L},\ x = \dfrac{\overline{x}}{L},\ u = \dfrac{\overline{u}}{U},\ v = \dfrac{\overline{v}}{\varepsilon U},\ \varepsilon = \dfrac{H}{L},\ \mu = \dfrac{\overline{\mu}}{\mu_0}e^{-\frac{E}{RT_w}}, T = \dfrac{E(\overline{T} - T_w)}{RT_w^2}, P = \dfrac{\varepsilon^2 L\overline{P}}{\mu_0 U}, \\ \beta = \dfrac{RT_w}{E}, Br = \dfrac{\mu_0 EU^2}{kRT_w^2}e^{-\frac{E}{RT_w}}, Pe = \dfrac{\rho c_p LU}{k}, \lambda = \dfrac{QC_0 AEH^2}{kRT_w^2}e^{-\frac{E}{RT_w}}, \mathrm{Re} = \dfrac{\rho UL}{\mu_0}, \end{array}\right\}$$

(3.2.7)

where μ, ρ, κ are the dynamic viscosity, fluid density and thermal conductivity respectively, *T* is the fluid temperature, T_w is the plate surface temperature, *u* is the axial velocity, *v* is the normal velocity, c_p is the specific heat at constant pressure, *p* is the pressure, *(x, y)* are distances measured in stream wise and normal direction respectively, *U* is the velocity scale, *Pe* is the Peclet number, β is the activation energy parameter, *Br* is the Brinkman number, λ is the Frank-Kamenetski parameter, *Re* is the Reynolds number. Since the channel aspect ratio is small ($0 < \varepsilon << 1$), the lubrication approximation based on an asymptotic simplification of the governing equations (**3.2.2)–(3.2.6)** is invoked. For Couette flow, the axial pressure gradient is zero (i.e. $\partial p / \partial x = 0$) and the flow is solely driven by the uniform motion of the upper plate. Equations **(3.2.2)-(3.2.6)** then become,

$$0 = \frac{\partial}{\partial y}\left(\mu\frac{\partial u}{\partial y}\right) + O\left(\varepsilon^2\right), \qquad \textbf{(3.2.8)}$$

$$0 = \frac{\partial p}{\partial y} + O\left(\varepsilon^2\right), \qquad \textbf{(3.2.9)}$$

$$0 = \frac{\partial^2 T}{\partial y^2} + \mu \mathrm{Br}\left(\frac{\partial u}{\partial y}\right)^2 + \lambda e^{\left(\frac{T}{1+\beta T}\right)} + O(\varepsilon^2). \qquad \textbf{(3.2.10)}$$

where $\mu = e^{-\frac{T}{(1+\beta T)}}$ .The appropriate boundary conditions in dimensionless form are given as follows:

$u = 0,\ T = 0$ (for a lower fixed impermeable plate) at $y = 0,$ **(3.2.11)**

$u = 1,\ T = 0,$ (the upper plate is subjected to a uniform motion) at $y = 1,$ **(3.2.12)**

Eqs. (3.2.8)– (3.2.10) subject to the boundary conditions can be easily combined to give

$$\frac{du}{dy} = me^{\frac{T}{(1+\beta T)}}, \quad \frac{d^2T}{dy^2} + \gamma e^{\frac{T}{(1+\beta T)}} = 0, \qquad \textbf{(3.2.13)}$$

where $\gamma = m^2 Br + \lambda$ and m is a constant to be determined. In the following sections, **Eq. (3.2.13)** is solved both analytically using a perturbation method and numerically using the standard Newton–Raphson shooting method along with a fourth-order Runge–Kutta integration algorithm [63].

3.3. Perturbation Approach

Due to the nonlinear nature of the velocity and temperature field equations in **(3.2.13)**, it is convenient to form a power series expansion both in the parameter γ i.e.,

$$u=\sum_{i=0}^{\infty}u_i\gamma^i, \quad T=\sum_{i=0}^{\infty}T_i\gamma^i. \qquad \textbf{(3.3.1)}$$

Substituting the solution series in **Eq. (3.3.1)** into **Eq. (3.2.13)** and collecting the coefficients of like powers of γ, we obtained the followings:

Order zero (γ^0)

$$\frac{du_0}{dy}=me^{\frac{T_0}{(1+\beta T_0)}}, \quad \frac{d^2T_0}{dy^2}=0,$$

with $u_0(0)=0$, $T_0(0)=0$, $u_0(1)=1$, $T_0(1)=0$,

Order one (γ^1)

$$\frac{du_1}{dy}=\frac{mT_1}{(1+\beta T_0)^2}e^{\frac{T_0}{(1+\beta T_0)}}, \quad \frac{d^2T_1}{dy^2}+e^{\frac{T_0}{(1+\beta T_0)}}=0,$$

with $u_1(0)=0$, $T_1(0)=0$, $u_1(1)=0$, $T_1(1)=0$,

Order two (γ^2)

$$\frac{du_2}{dy}=-\frac{me^{\frac{T_0}{(1+\beta T_0)}}}{2(1+\beta T_0)^4}(2T_1^2\beta+2T_0T_1^2\beta^2-T_1^2-2T_2-4T_0T_2\beta-2T_2T_0^2\beta^2),$$

$$\frac{d^2T_2}{dy^2}+\frac{T_1}{(1+\beta T_0)^2}e^{\frac{T_0}{(1+\beta T_0)}}=0,$$

with $u_2(0)= 0$, $T_2(0) = 0$, $u_2(1)= 0$, $T_2(1) = 0$,

and so on. The above equations for the coefficients of solution series are solved iteratively for the velocity and temperature fields and we obtain;

$$T(y) = -\frac{1}{2} y (y-1) \gamma + \frac{1}{24} y (y-1) (y^2 - y - 1) \gamma^2 + \frac{1}{1440} y (y-1) (12\beta y^4 - 8y^4 - 24\beta y^3 + 16y^3 + 6\beta y^2 + y^2 - 9y + 6y\beta - 9 + 6\beta) \gamma^3 + O(\gamma^4) \quad \textbf{(3.3.2)}$$

$$u(y) = y - \frac{1}{12} y (2y-1) (y-1) \gamma - \frac{1}{360} y (2y-1) (y-1) (3y^2 - 3y - 1) (-2 + 3\beta) \gamma^2 - \frac{1}{60480} y (2y-1) (y-1) (-756\beta y^4 + 540\beta^2 y^4 + 204y^4 - 1080y^3 \beta^2 - 408y^3 + 1512\beta y^3 + 63y^2 - 378\beta y^2 + 378y^2 \beta^2 + 141y + 162y\beta^2 - 378y\beta + 54\beta^2 + 47 - 126\beta) \gamma^3 + O(\gamma^4) \quad \textbf{(3.3.3)}$$

It is noteworthy that in the limit of $\gamma \to 0$, the fluid velocity profile obtained in **Eq. (3.3.3)** reduces to $u(y) = y$ which corresponds to the classical linear velocity profile for Couette flow with constant fluid viscosity. Using a computer symbolic algebra package (MAPLE) [63], the first few terms of the above solution series in **Eqs. (3.3.2) - (3.3.3)** are obtained. We are aware that these power series solutions are valid for very small parameter values. However, using Hermite-Padé approximation technique, we have extended the usability of the solution series beyond small parameter values as illustrated in the following section.

3.4. Hermite-Padé Approximation Technique

From the application point of view, it is extremely important to determine the appearance of criticality or non-existence of steady-state solution for certain parameter values. In order to achieve this, we first derived a special type of Hermite-Padé approximant. Let

$$U_N(\gamma) = \sum_{n=0}^{N} a_n \gamma^n + O(\gamma^{N+1}), \qquad \text{as} \quad \gamma \to 0, \tag{3.4.1}$$

be a given partial sum. It is important to note here that **Eq. (3.4.1)** can be used to approximate any output of the solution of the problem under investigation (e.g. the series for the wall heat flux parameter in terms of Nusselt number $Nu = -dT/dy$ at $y = 1$), since everything can be Taylor expanded in the given small parameter. Assume $U(\gamma)$ is a local representation of an algebraic function of γ in the context of nonlinear problems, we seek an expression of the form

$$F_d(\gamma, U) = \sum_{m=1}^{d} \sum_{k=0}^{m} f_{m-k,k} \gamma^{m-k} U^k, \tag{3.4.2}$$

of degree $d \geq 2$, such that

$$\frac{\partial F_d}{\partial U}(0,0) = 1 \text{ and } F_d(\gamma, U_N) = O(\gamma^{N+1}), \quad \text{as} \quad \gamma \to 0. \tag{3.4.3}$$

The requirement **(3.4.3)** reduces the problem to a system of N linear equations for the unknown coefficients of F_d. The entries of the underlying matrix depend only on the N given coefficients a_n and we shall take $N = (d^2 + 3d - 2)/2$, so that the number of equations equals the number of unknowns. The polynomial F_d is a special type of Hermite-Padé approximant and is then investigated for bifurcation and criticality conditions using Newton diagram, Vainberg and Trenogin [77].

3.4. Numerical Approach

The numerical technique chosen for the solution of the coupled ordinary differential **Eq. (3.2.13)** is the standard Newton–Raphson shooting method along with a fourth-order Runge–Kutta integration algorithm. **Eq. (3.2.13)** is transformed into a system of first order differential equations as follows. Let $u = x_1$, $T = x_2$, $T' = x_3$, where the prime symbol represent derivatives with respect to *y*. Then, the problem becomes,

$$x_1' = me^{\frac{x_2}{(1+\beta x_2)}},\ x_2' = x_3,\ x_3' = -\gamma e^{\frac{x_2}{(1+\beta x_2)}}, \qquad \textbf{(3.5.1)}$$

subject to the following initial conditions,

$$x_1(0) = 0,\ x_2(0) = 0,\ x_3(0) = s_1. \qquad \textbf{(3.5.2)}$$

The unspecified initial condition s_1 and the undetermined constant *m* are guessed systematically and **Eq. (3.5.1)** is then integrated numerically as initial value problem to the given terminal point at *y* =1. For each set of parameter values for β and γ, the procedure is repeated until conditions at the *y* =1 (i.e. $x_1(1) = 1$, $x_2(1) = 0$) are satisfied and the desired degree of accuracy (namely 10^{-7}) of the results obtained is achieved.

3.4. Entropy Analysis

Flow and heat transfer processes between two parallel plates are irreversible. The non-equilibrium conditions arise due to the exchange of energy and momentum within the fluid and at solid boundaries, thus resulting in entropy generation. Apart of the entropy production is due to the heat transfer in the direction of finite temperature gradients and

the other part of entropy production arises due to the fluid friction. The general equation for the entropy generation per unit volume is given by [9, 10, 43, 60],

$$S^m = \frac{k}{T_w^2}\left(\nabla \bar{T}\right)^2 + \frac{\mu}{T_w}\Phi . \qquad \textbf{(3.6.1)}$$

The first term in equation **(3.6.1)** is the irreversibility due to heat transfer and the second term is the entropy generation due to viscous dissipation. Using equation **(3.6.1)**, we express the entropy generation number in dimensionless form as,

$$Ns = \frac{H^2 E^2 S^m}{kR^2 T_w^2} = \left(\frac{\partial T}{\partial y}\right)^2 + \frac{\mu Br}{\beta}\left(\frac{\partial u}{\partial y}\right)^2 + O(\varepsilon^2), \qquad \textbf{(3.6.2)}$$

In equation **(3.6.2)**, the first term can be assigned as N_1 and the second term due to viscous dissipation as N_2, i.e.

$$N_1 = \left(\frac{\partial T}{\partial y}\right)^2, \quad N_2 = \frac{\mu Br}{\beta}\left(\frac{\partial u}{\partial y}\right)^2 . \qquad \textbf{(3.6.3)}$$

In order to have an idea whether fluid friction dominates over heat transfer irreversibility or vice-versa, Bejan [4] defined the irreversibility distribution ratio as $\Phi = N_2/N_1$. Heat transfer dominates for $0 \leq \Phi < 1$ and fluid friction dominates when $\Phi > 1$. The contribution of both heat transfer and fluid friction to entropy generation are equal when $\Phi = 1$. In many engineering designs and energy optimisation problems, the contribution of heat transfer entropy N_1 to overall entropy generation rate Ns is needed. As an alternative to irreversibility parameter, the Bejan number (*Be*) is define mathematically as

$$Be = \frac{N_1}{Ns} = \frac{1}{1+\Phi} \quad . \qquad \textbf{(3.6.4)}$$

Clearly, the Bejan number ranges from 0 to 1. *Be* = 0 is the limit where the irreversibility is dominated by fluid friction effects and *Be* = 1 corresponds to the limit where the irreversibility due to heat transfer by virtue of finite temperature differences dominates. The contribution of both heat transfer and fluid friction to entropy generation are equal when *Be* = 1/2.

3.7. Results and Discussion

We emphasis here that an increase in the parameter value of β indicates an increase in the fluid viscosity and a decrease in the fluid activation energy while an increase in the parameter value of γ signifies an increase in the reactive flow Arrhenius kinetics. **Table (3.7.1)** below demonstrates agreement between the results obtained using perturbation technique and purely fourth-order Runge–Kutta numerical integration approach coupled with shooting method at small and moderate parameter values. Generally, the difference is of order 10^{-8}.

Table 3.7.1: Comparison between analytical and numerical results ($\beta = 0.1$, $\gamma = 0.5$)

y	$T(y)$ Perturbation Results	$T(y)$ Numerical Results	$\lvert T_{numer.} - T_{perturb.} \rvert$
0	0	0	0
0.1	0.02360044943	0.02360039520	5.423×10^{-8}
0.2	0.04208380022	0.04208374384	5.638×10^{-8}
0.3	0.05535532038	0.05535525228	6.810×10^{-8}
0.4	0.06334613033	0.06334604947	8.086×10^{-8}
0.5	0.06601440811	0.06601432697	8.114×10^{-8}
0.6	0.06334613023	0.06334604947	8.076×10^{-8}
0.7	0.05535532037	0.05535525228	6.809×10^{-8}
0.8	0.04208380020	0.04208374384	5.636×10^{-8}
0.9	0.02360044944	0.02360039520	5.424×10^{-8}
1.0	0	0	0

The Hermite-Padé approximation procedure in **section (3.1.4)** above was applied to the first few terms of the solution series in **section (3.2)** and we obtained the results as shown in **tables (3.7.2)** and **(3.7.3)** below:

Table 3.7.2: Computations showing the criticality procedure rapid convergence (β = 0.1).

D	N	Nu	γ_{cN}
2	4	5.0854548671499	3.9528766995579
3	8	5.0849831249732	3.9528312115207
4	13	5.0849831815807	3.9528312148390
5	19	5.0849831815664	3.9528312148383
6	26	5.0849831815664	3.9528312148383

Table 3.7.3: Computations showing thermal criticality for different parameter values

β	0	0.1	0.15	0.2
Nu	4.0000000000000	5.0849831815664	6.0215731738934	7.7178156381921 41
γ_c	3.5138307191251 6	3.9528312148383	4.2506038264647	4.6479180091289 50

The results in **table (3.7.2)** reveal the rapid convergence of Hermite-Padé approximation procedure with gradual increase in the number of series coefficients utilized in the approximants. In **table (3.7.3)**, it is noteworthy that the magnitude of thermal criticality (γ_c) increases with an increase in the reactive flow activation energy parameter (i.e. β >> 0). This invariably will lead to a delay in the development of thermal runaway in the flow system and enhance flow thermal stability.

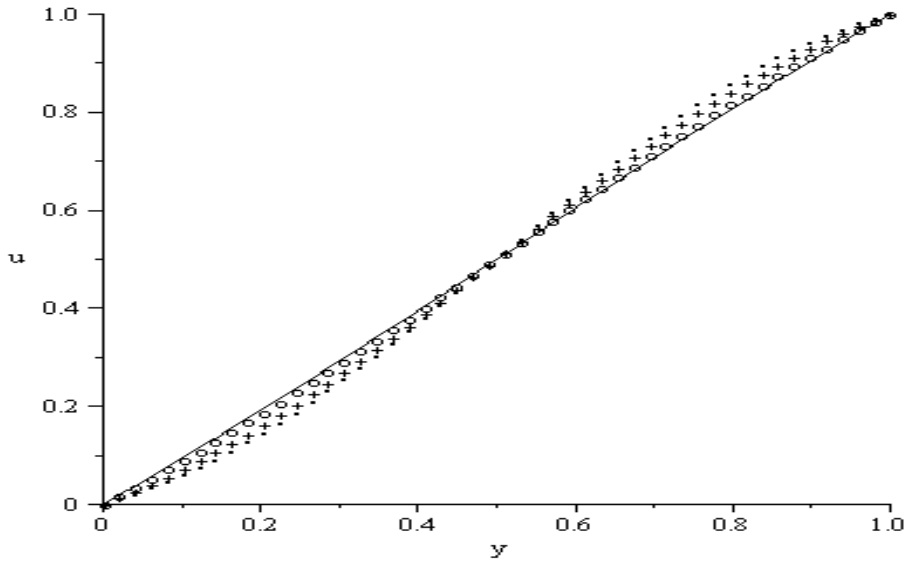

Fig.3.7.2. Velocity profile: $\beta = 0.3$; _____ $\gamma = 1$; ooooo $\gamma = 2$; ++++ $\gamma = 4$; …… $\gamma = 5$.

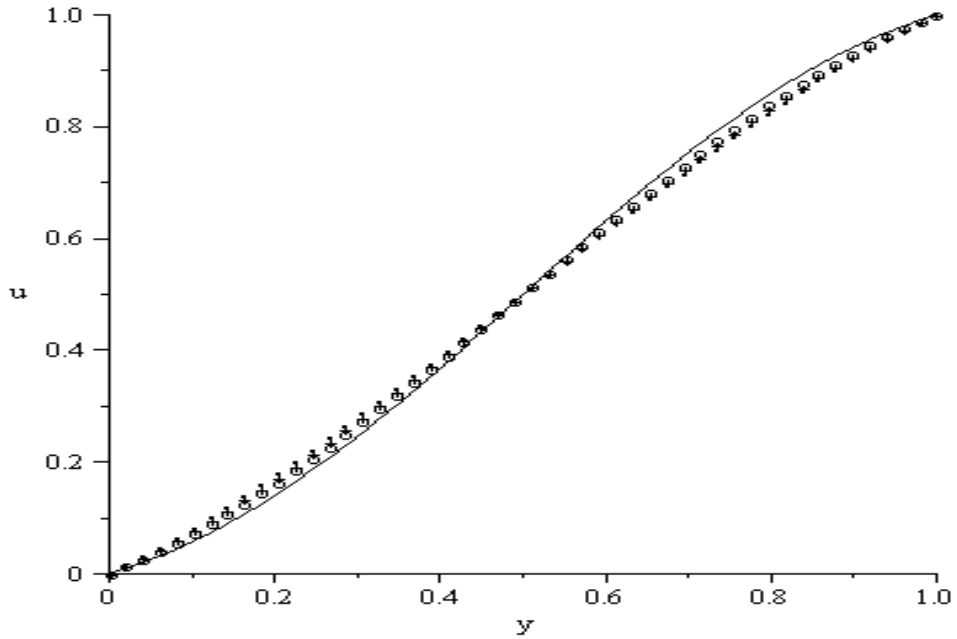

Fig.3.7.3. Velocity profile: $\gamma = 5$; _____ $\beta = 0.3$; ooooo $\beta = 0.5$; ++++ $\beta = 0.7$; …... $\beta = 1$.

The velocity profiles are reported for increasing values of γ and β in **Figs. 3.7.2 - 3.7.3.** The fluid velocity is zero at the lower stationary plate and increases gradually towards the upper moving upper plate. For $\gamma = 0$, the fluid shows the standard Couette linear velocity profile with maximum velocity at the moving upper plate. As the parameter value of $\gamma > 0$ increases, the Arrhenius kinetic increases, causing the velocity profile to increase nonlinearly across the channel to a maximum at y =1. Furthermore, for increasing value of β, an inflexion point appears in the velocity profile around the centre of the channel as shown in **Fig. 3.7.3**.

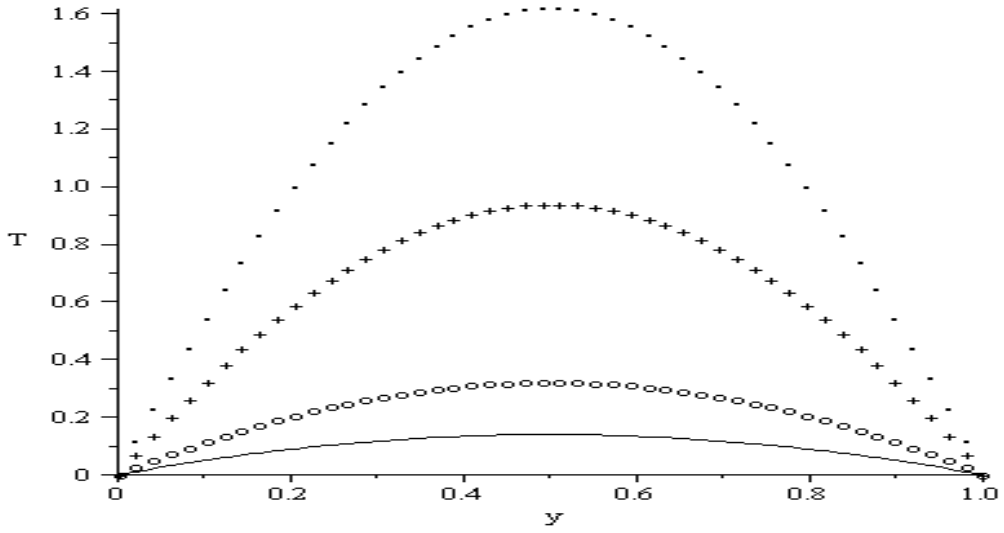

Fig.3.7.4. Temperature profile: β = 0.3; _____ γ = 1; ooooo γ= 2; ++++ γ= 4; …… γ= 5.

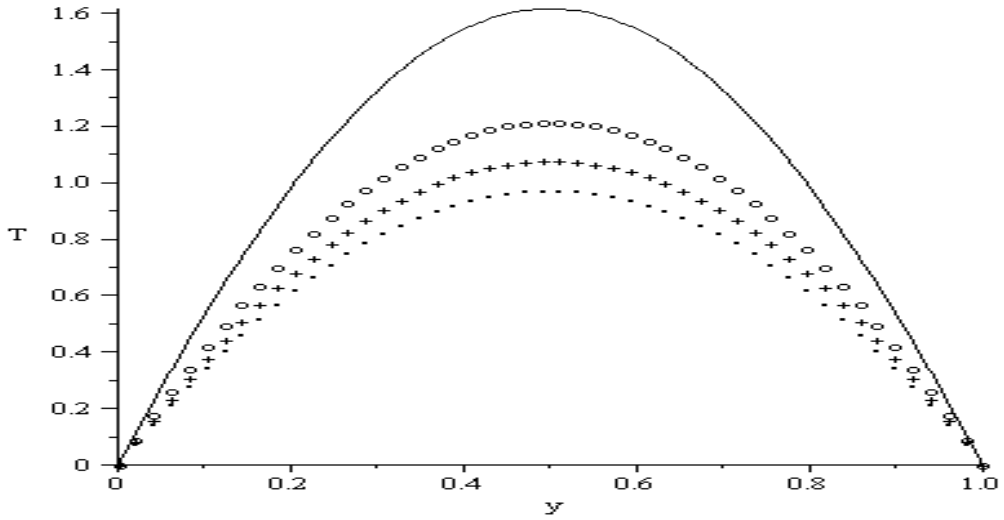

Fig.3.7.5. Temperature profile: γ=5; ___β = 0.3; oooo β= 0.5; ++++ β = 0.7; ….β = 1.

Typical variations of the fluid temperature profiles in the normal direction are shown in **Figs. 3.7.4-3.7.5**. The fluid temperature increases with increasing values ofλ. This can be attributed to an increase in heat generation within the fluid due to exothermic reaction as illustrated in **Fig. 3.7.4**. A decrease in the fluid temperature is observed when the parameter value of β increases, in this case, the fluid activation energy is reduced and its viscosity has increased. Meanwhile, minimum temperature is generally observed at both the lower and the upper plate surfaces while the maximum temperature occurs around the core region of the channel.

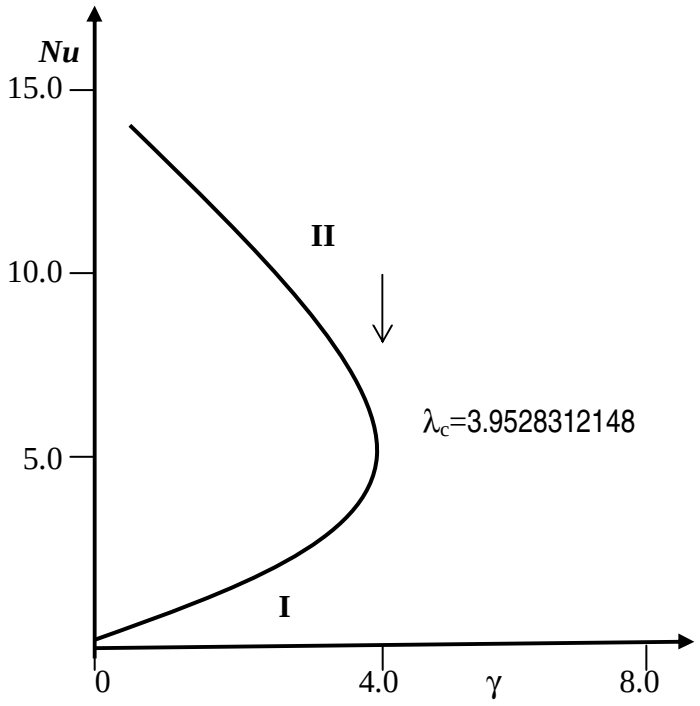

Fig. 3.7. 6. A slice of approximate bifurcation diagram in the (γ , *Nu* (β = 0.1)) plane

A slice of the bifurcation diagram for $0<\beta << 1$ in the (γ, *Nu*) plane is shown in **Fig.3.7.6**. It represents the qualitative change in the flow system as the parameter (γ) increases. In particular, for $0\leq\beta <<1$ there is a critical value γ_c (a turning point) such that, for $0 < \gamma < \gamma_c$ there are two solutions (labelled **I** and **II**). The upper and lower solution branches occur due to the temperature dependent variable viscosity and Arrhenius kinetics in the governing thermal boundary layer equation **(Eq. 3.2.13)**. When $\gamma > \gamma_c$ the system has no real solution and displays a classical form indicating thermal runaway. As temperature increases the fluid viscosity decreases exponentially. The velocity gradient specified by **Eq. (3.2.13)**, increases exponentially with temperature coupled with increasing Arrhenius kinetics and feeds back into the temperature equation, leading to thermal runaway.

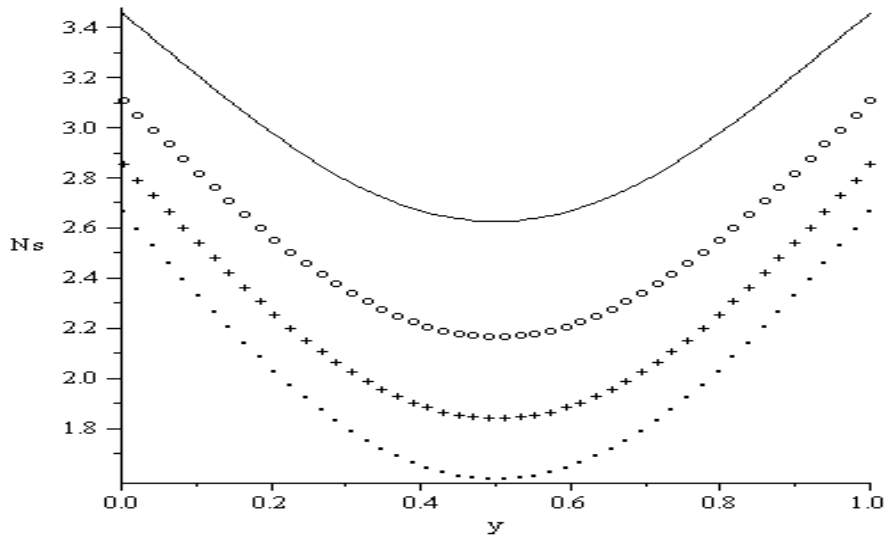

Fig. 3.7.7. Entropy generation rate: γ=2; ____β = 0.5; ooooo β= 0.6; ++++ β = 0.7; …..β = 0.8

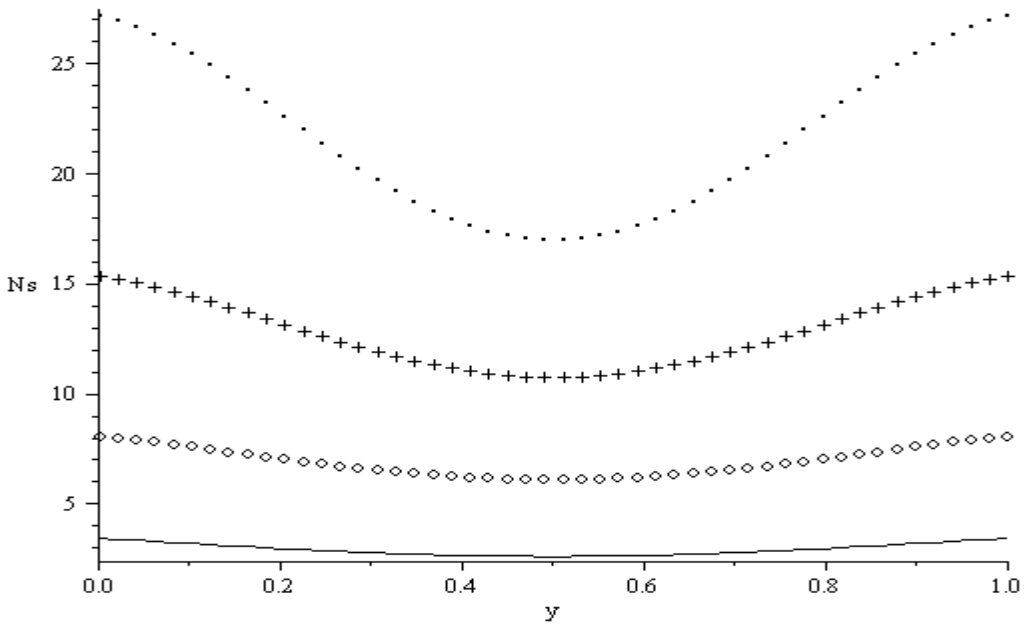

Fig. 3.7.8. Entropy generation rate: β = 0.5; _____ γ = 2; oooooγ = 3; ++++ γ = 4; ……γ= 5.

Figs. 3.7.7-3.7.8 display results for the entropy generation versus the channel width for various parametric values. Generally, entropy generation rate is maximum at the plate surfaces and minimum around the core region of the channel. It is interesting to note that the entropy generation rate decreases with increasing value β and increases with increasing value of γ.

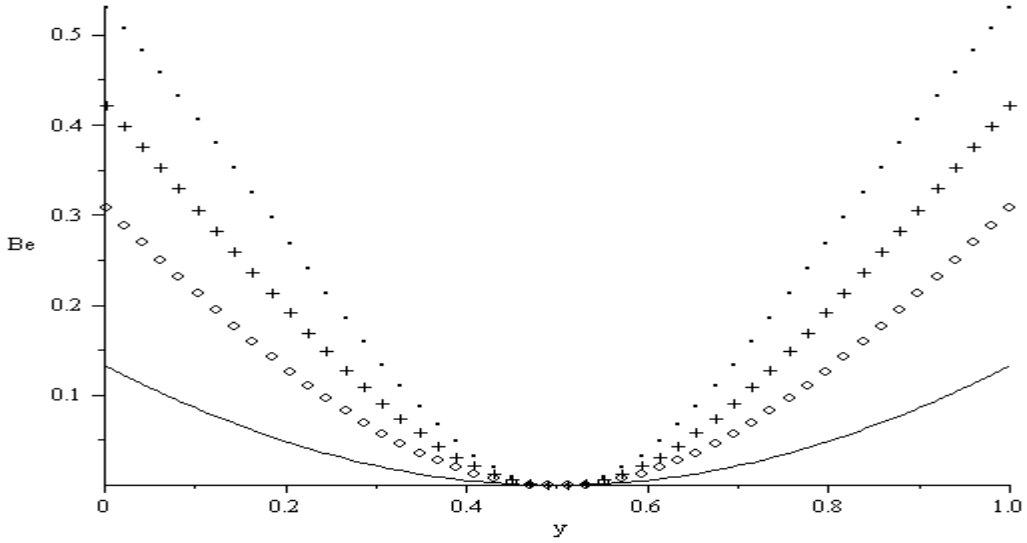

Fig. 3.7.9. Bejan number: γ=2; _____β = 0.1; ooooo β= 0.3; ++++ β = 0.5; …...β = 0.8

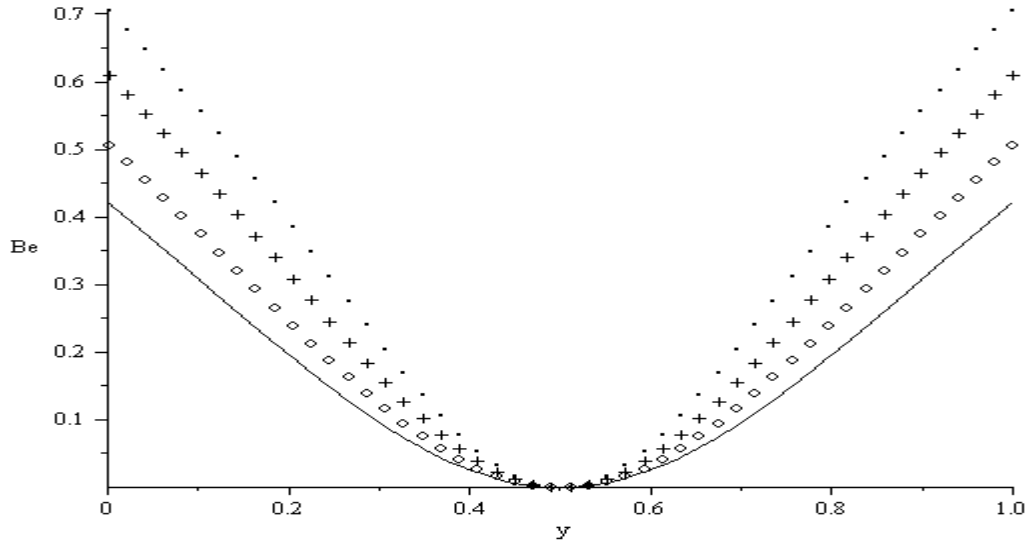

Fig. 3.7.10. Bejan number: $\beta = 0.5$; _____ $\gamma = 2$; ooooo $\gamma = 3$; ++++ $\gamma = 4$; …… $\gamma = 5$.

Figs. 3.7.9-3.7.10 display the Bejan (*Be*) number versus the channel width. It is observed that the fluid friction irreversibility dominates at the channel core region while the heat transfer irreversibility dominates at the both lower and upper plate surfaces. The dominant effect of heat transfer irreversibility at the plate increases with increasing values of β and γ.

CHAPTER

4

ENTROPY ANALYSIS FOR A VARIABLE VISCOSITY REACTIVE POISEUILLE FLOW

4.1. Introduction

The phenomenon of the flow and heat transfer in a channel has been analyzed by a number of authors [34, 60, 62] due to its important applications in the fields related to thermal power plants, heat exchangers, electronic cooling devices, fluidization, combustion, petroleum industry, physiological flow system, polymer technology, etc. However, most fluids used in engineering and industrial systems can be subjected to extreme conditions, such as high temperature, pressure and shear rate. External heating and high shear rates can lead to high temperature being generated within the fluid. This may have a significant effect on the fluid properties. It is well known that the most sensitive fluid property to temperature rise is the viscosity [52, 53]. For example, when the temperature increases from 10^{o}C ($\bar{\mu}$ = 0.0131g/cm s) to 50^{o}C ($\bar{\mu}$ = 0.00548 g/cm s), the viscosity of water decreases by 240% [34, 60].

Meanwhile the inclusion of entropy generation calculations in computational fluid dynamics problems allows the evaluation of local entropy generation in more complicated thermal phenomena. One theoretically correct measure of thermodynamic performance is the magnitude of thermodynamic irreversibility's associated with a component or process. It can be shown that the minimization of entropy generation also results in the maximum reduction of irreversibility. The development of improved thermal designs is enhanced by the ability to identify clearly the source and location of

entropy generation. Many studies have been published to assess the sources of irreversibility in components and systems. Bejan [9] studied the entropy generation for forced convective heat transfer due to temperature gradient and viscosity effect in a fluid. Bejan [10] also presented various reasons behind entropy generation in applied thermal engineering where the generation of entropy destroys the available work, called exergy, of a system. Entropy generation in a vertical concentric isothermal channel with temperature dependent viscosity is presented by Tasnim and Mahmud [53]. The inherent irreversibility for a gravity driven non-Newtonian Ostwald-de Waele power law liquid film along an inclined isothermal plate is discussed in Makinde [42]. The thermodynamics second law characteristics for thermal design of radial fin geometry by convection are discussed by Taufiq et al. [67]. Other applications of second law analysis for some steady flow devices can be found in references [33, 66].

Considering the importance of variable viscosity and Arrhenius kinetic effects on entropy generation rate, the problem of inherent irreversibility in the flow of a reactive variable viscosity fluid through a channel with parallel plates that is subjected to Arrhenius kinetic is studied. The nonlinear governing equations are solved both analytically and numerically using perturbation technique and the standard Newton–Raphson shooting method along with a fourth-order Runge–Kutta integration algorithm in order to obtain the fluid velocity and temperature profiles. The volumetric entropy generation rate, irreversibility distribution ratio and the Bejan number are also obtained. The results are presented graphically and discussed quantitatively with appropriate physical explanations.

4.2. Problem Formulation

The configuration of the problem studied in this chapter is depicted in **Fig. 4.2.1** The fluid is assumed to be viscous, incompressible, reactive and flowing steadily in the $\bar{x}$-direction under the action of a constant pressure gradient through a channel with parallel plates of width $2H$ and length L. Following [2, 60] the temperature dependent viscosity ($\bar{\mu}$) and the chemical reaction kinetic (G) functions can be expressed in Arrhenius type [34, 60, 62] as

$$\overline{\mu} = \mu_0 e^{\frac{E}{\overline{RT}}}, \quad G = QC_0 Ae^{-\frac{E}{\overline{RT}}} \qquad \textbf{(4.2.1)}$$

where E is the activation energy, R is the universal gas constant, Q is the heat of reaction, A is the rate constant, C_0 is the initial concentration of the reactant species and μ_0 is the fluid reference dynamic viscosity at a very large temperature (i.e. as $\overline{T} \to \infty$).

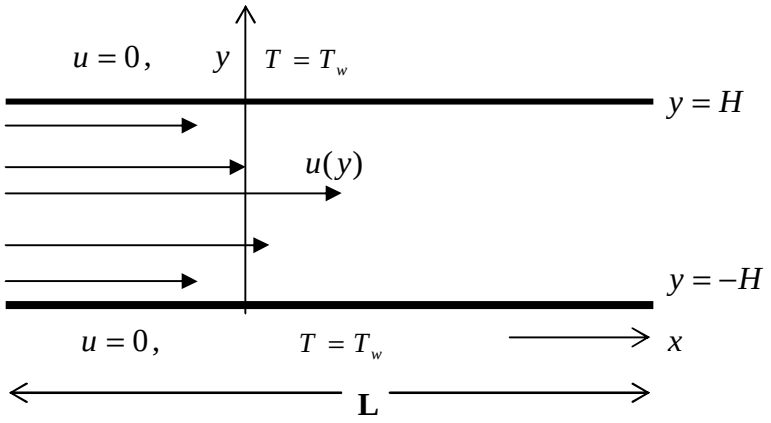

Fig. 4.2.1: Schematic diagram of the problem

Under these conditions the continuity, momentum and energy equations governing the problem in dimensionless form may be written as [34, 42, 43, 60];

$$\frac{\partial u}{\partial x} + \frac{\partial v}{\partial y} = 0, \qquad \textbf{(4.2.2)}$$

$$Re^2 \left(u\frac{\partial u}{\partial x} + v\frac{\partial u}{dy} \right) = -\frac{\partial p}{\partial x} + 2\varepsilon^2 \frac{\partial}{\partial x}\left(\mu \frac{\partial u}{\partial x} \right) + \frac{\partial}{\partial y}\left[\mu \left(\frac{\partial u}{\partial y} + \varepsilon^2 \frac{\partial v}{\partial x} \right) \right], \qquad \textbf{(4.2.3)}$$

$$Re^4 \left(u\frac{\partial v}{\partial x} + v\frac{\partial v}{\partial y} \right) = -\frac{\partial p}{\partial y} + 2\varepsilon^2 \frac{\partial}{\partial y}\left(\mu \frac{\partial v}{\partial y} \right) + \varepsilon^2 \frac{\partial}{\partial x}\left[\mu \left(\frac{\partial u}{\partial y} + \varepsilon^2 \frac{\partial v}{\partial x} \right) \right], \qquad \textbf{(4.2.4)}$$

$$\varepsilon^2 Pe\left(u\frac{\partial T}{\partial x}+v\frac{\partial T}{\partial y}\right)=\varepsilon^2\frac{\partial^2 T}{\partial x^2}+\frac{\partial^2 T}{\partial y^2}+\lambda e^{\left(\frac{T}{1+\beta T}\right)}+\mu\Phi, \qquad \textbf{(4.2.5)}$$

where

$$\Phi=\mathrm{Br}\left[2\varepsilon^2\left(\frac{\partial u}{\partial x}\right)^2+2\varepsilon^2\left(\frac{\partial v}{\partial y}\right)^2+\left(\frac{\partial u}{\partial y}+\varepsilon^2\frac{\partial v}{\partial x}\right)^2\right]. \qquad \textbf{(4.2.6)}$$

We have employed the following non-dimensional quantities in **Eqs. (4.2.2)-(4.2.6):**

$$\begin{aligned}
&y=\frac{\bar{y}}{\varepsilon L}, x=\frac{\bar{x}}{L}, u=\frac{\bar{u}}{U}, v=\frac{\bar{v}}{\varepsilon U}, \varepsilon=\frac{H}{L}, \mu=\frac{\bar{\mu}}{\mu_0}e^{-\frac{E}{RT_w}}, T=\frac{E(\bar{T}-T_w)}{RT_w^2},\\
&P=\frac{\varepsilon^2 L\bar{P}}{\mu_0 U}, \beta=\frac{RT_w}{E}, Br=\frac{\mu_0 EU^2}{kRT_w^2}e^{-\frac{E}{RT_w}}, Pe=\frac{\rho c_p LU}{k},\\
&\lambda=\frac{QC_0 AEH^2}{kRT_w^2}e^{-\frac{E}{RT_w}}, \mathrm{Re}=\frac{\rho UL}{\mu_0}, \gamma=\frac{BrG^2 kRT_w^2}{QC_0 AEH^2}e^{\frac{E}{RT_w}},
\end{aligned} \qquad \textbf{(4.2.7)}$$

where μ, ρ, κ are the dynamic viscosity, fluid density and thermal conductivity respectively, T is the fluid temperature, T_w is the plate surface temperature, u is the axial velocity, v is the normal velocity, c_p is the specific heat at constant pressure, p is the pressure, (x, y) are distances measured in streamwise and normal direction respectively, U is the velocity scale, Pe is the Peclet number, β is the activation energy parameter, Br is the Brinkman number, λ is the Frank-Kamenetski parameter, Re is the Reynolds number. Since the channel aspect ratio is small ($0 < \varepsilon << 1$), the lubrication approximation based on an asymptotic simplification of the governing equations **(4.2.2)–(4.2.6)** is invoked. For Poiseuille flow, the axial pressure gradient is constant (i.e. $-\partial p/\partial x = G$) and the flow is solely driven by the constant axial pressure gradient. **Eqs. (4.2.2)-(4.2.6)** then become,

$$0=G+\frac{\partial}{\partial y}\left(\mu\frac{\partial u}{\partial y}\right)+O\left(\varepsilon^2\right), \qquad \textbf{(4.2.8)}$$

$$0=\frac{\partial p}{\partial y}+O\left(\varepsilon^2\right), \qquad \textbf{(4.2.9)}$$

$$0 = \frac{\partial^2 T}{\partial y^2} + \mu \mathrm{Br}\left(\frac{\partial u}{\partial y}\right)^2 + \lambda e^{\left(\frac{T}{1+\beta T}\right)} + O(\varepsilon^2). \qquad \textbf{(4.2.10)}$$

where $\mu = e^{-\frac{T}{(1+\beta T)}}$. The appropriate boundary conditions in dimensionless form are given as follows: the channel surface is fixed and impermeable:

$$u = 0,\ T = 0 \qquad \text{at} \quad y = 1, \qquad \textbf{(4.2.11)}$$

and the symmetry condition along the centerline i.e.

$$\frac{du}{dy} = \frac{dT}{dy} = 0, \qquad \text{at} \quad y = 0. \qquad \textbf{(4.2.12)}$$

Eqs.(4.2.8)–(4.2.10) subject to the boundary conditions can be easily combined to give

$$\frac{du}{dy} = -yGe^{\frac{T}{(1+\beta T)}}, \quad \frac{d^2T}{dy^2} + \lambda(1+\gamma y^2)\, e^{\frac{T}{(1+\beta T)}} = 0, \qquad \textbf{(4.2.13)}$$

where γ is the viscous dissipation parameter. In the following sections, **Eq. (4.2.13)** is solved analytically and numerically using perturbation technique and the standard Newton–Raphson shooting method along with a fourth-order Runge–Kutta integration algorithm [, 14].

4.1.1. Perturbation Approach

Due to the nonlinear nature of the velocity and temperature field equations in **(4.2.13)**, it is convenient to form a power series expansion both in the parameter λ i.e.

$$u = \sum_{i=0}^{\infty} u_i \lambda^i, \quad T = \sum_{i=0}^{\infty} T_i \lambda^i. \qquad \textbf{(4.3.1)}$$

Substituting the solution series in **Eq. (4.3.1)** into **Eq. (4.2.13)** and collecting the coefficients of like powers of λ, we obtained the followings:

Order zero (λ^0)

$$\frac{du_0}{dy} = -Gye^{\frac{T_0}{(1+\beta T_0)}}, \quad \frac{d^2T_0}{dy^2} = 0,$$

with

$$u_0(1) = 0,\ T_0(1) = 0,\ \frac{du_0}{dy}(0) = \frac{dT_0}{dy}(0) = 0,$$

Order one (λ^1)

$$\frac{du_1}{dy} = -\frac{yGT_1}{(1+\beta T_0)^2}e^{\frac{T_0}{(1+\beta T_0)}}, \quad \frac{d^2T_1}{dy^2} + (1+\gamma y^2)e^{\frac{T_0}{(1+\beta T_0)}} = 0,$$

with

$$u_1(1) = 0,\ T_1(1) = 0,\ \frac{du_1}{dy}(0) = \frac{dT_1}{dy}(0) = 0$$

Order two (λ^2)

$$\frac{du_2}{dy} = \frac{yGe^{\frac{T_0}{(1+\beta T_0)}}}{2(1+\beta T_0)^4}(2T_1^2\beta + 2T_0T_1^2\beta^2 - T_1^2 - 2T_2 - 4T_0T_2\beta - 2T_2T_0^2\beta^2),$$

$$\frac{d^2T_2}{dy^2} + \frac{(1+\gamma y^2)T_1}{(1+\beta T_0)^2}e^{\frac{T_0}{(1+\beta T_0)}} = 0,$$

with

$$u_2(1) = 0,\ T_2(2) = 0,\ \frac{du_2}{dy}(0) = \frac{dT_2}{dy}(0) = 0,$$

and so on. The above equations for the coefficients of solution series are solved iteratively for the velocity and temperature fields and we obtain;

$$\begin{aligned} T(y) =& -\frac{1}{12}\lambda\left(y^2-1\right)\left(\gamma y^2+6+\gamma\right)+\frac{1}{10080}\lambda^2\left(y^2\right.\\ &\left.-1\right)\left(15y^6\gamma^2+196\gamma y^4+15\gamma^2y^4-55y^2\gamma^2+420y^2\right.\\ &\left.-224\gamma y^2-644\gamma-2100-55\gamma^2\right)+\frac{1}{9979200}\lambda^3\left(y^2-1\right)\left(\right.\\ &-1302840-581130\gamma+10010\beta\gamma^2y^8-134640\beta\gamma y^4\\ &+525y^{10}\beta\gamma^3-1950y^6\beta\gamma^3+3825y^2\beta\gamma^3+7524y^6\gamma^2\\ &-47916y^2\gamma^2-375\gamma^3y^8+2100\gamma^3y^4+525\beta\gamma^3y^8\\ &-1950\beta\gamma^3y^4+32120\beta y^2\gamma^2-92466\gamma^2+153450\gamma y^4\\ &-55440y^4-375\gamma^3y^{10}-5325\gamma^3+3825\beta\gamma^3+83160\beta y^4\\ &-332640\beta y^2+419760\beta\gamma+66770\beta\gamma^2-37180\beta\gamma^2y^4\\ &+59400\beta y^6\gamma+3960\beta y^2\gamma-40590y^6\gamma-7326\gamma^2y^8\\ &+39864\gamma^2y^4-54450\gamma y^2+360360y^2-4840\beta y^6\gamma^2\\ &+914760\beta+2100\gamma^3y^6-5325\gamma^3y^2\left.\right)+O\left(\lambda^4\right) \end{aligned} \qquad \textbf{(4.3.2)}$$

$$\begin{aligned} u(y) =& -\frac{1}{2}G\left(y^2-1\right)+\frac{1}{72}\lambda G\left(y^2-1\right)^2\left(\gamma y^2+9+2\gamma\right)\\ &+\frac{1}{30240}\lambda^2G\left(y^2-1\right)^2\left(-15y^6\gamma^2+21\beta y^6\gamma^2+315\beta\gamma y^4\right.\\ &-231\gamma y^4-30\gamma^2y^4+42\beta\gamma^2y^4+1260\beta y^2+25y^2\gamma^2\\ &-42\gamma y^2+210\beta y^2\gamma-7\beta y^2\gamma^2-840y^2+2100+80\gamma^2\\ &\left.-525\beta\gamma-56\beta\gamma^2+777\gamma-1260\beta\right)+O\left(\lambda^3\right) \end{aligned} \qquad \textbf{(4.3.3)}$$

It is noteworthy that in the limit of $\lambda \to 0$, the fluid velocity profile obtained in **Eq. (4.3.3)** reduces to $u(y) = G(1-y^2)/2$ which corresponds to the classical parabolic velocity profile for plane-Poiseuille flow with constant fluid viscosity. Using a computer symbolic algebra package (MAPLE) [63], the first few terms of the above solution series in **Eqs. (4.3.2) - (4.3.3)** are obtained. We are aware that these power series solutions are valid for very small parameter values. However, using Hermite-Padé approximation technique, we have extended the usability of the solution series beyond small parameter values as illustrated in the following section.

4.4. Hermite-Padé Approximation Technique

From the application point of view, it is extremely important to determine the appearance of criticality or non-existence of steady-state solution for certain parameter values. In order to achieve this, we first derived a special type of Hermite-Padé approximant. Let

$$U_N(\lambda) = \sum_{n=0}^{N} a_n \lambda^n + O(\lambda^{N+1}), \qquad \text{as } \lambda \to 0, \qquad \textbf{(4.4.1)}$$

be a given partial sum. It is important to note here that **Eq. (4.4.1)** can be used to approximate any output of the solution of the problem under investigation (e.g. the series for the wall heat flux parameter in terms of Nusselt number $Nu = -dT/dy$ at $y = 1$), since everything can be Taylor expanded in the given small parameter. Assume $U(\lambda)$ is a local representation of an algebraic function of γ in the context of nonlinear problems, we seek an expression of the form

$$F_d(\gamma, U) = \sum_{m=1}^{d} \sum_{k=0}^{m} f_{m-k,k} \lambda^{m-k} U^k, \qquad \textbf{(4.4.2)}$$

of degree $d \geq 2$, such that

$$\frac{\partial F_d}{\partial U}(0,0) = 1 \text{ and } F_d(\lambda, U_N) = O(\lambda^{N+1}), \qquad \text{as} \quad \lambda \to 0. \qquad \textbf{(4.4.3)}$$

The requirement **(4.4.3)** reduces the problem to a system of N linear equations for the unknown coefficients of F_d. The entries of the underlying matrix depend only on the N given coefficients a_n and we shall take $N = (d^2 + 3d - 2)/2$, so that the number of equations equals the number of unknowns. The polynomial F_d is a special type of Hermite-Padé approximant and is then investigated for bifurcation and criticality conditions using Newton diagram, Vainberg and Trenogin [16].

4.5. Numerical Approach

The numerical technique chosen for the solution of the coupled ordinary differential **Eq. (4.2.13)** is the standard Newton–Raphson shooting method along with a fourth-order Runge–Kutta integration algorithm. **Eq. (4.2.13)** is transformed into a system of first order differential equations as follows. Let $u = x_1$, $T = x_2$, $T' = x_3$, where the prime symbol represent derivatives with respect to *y*. Then, the problem becomes,

$$x_1' = -yGe^{\frac{x_2}{(1+\beta x_2)}},\ x_2' = x_3,\ x_3' = -\lambda(1+\gamma y^2)e^{\frac{x_2}{(1+\beta x_2)}}, \qquad \textbf{(4.5.1)}$$

subject to the following initial conditions,

$$x_1(0) = s_1, x_2(0) = s_2, x_3(0) = 0. \qquad \textbf{(4.5.2)}$$

The unspecified initial conditions s_1 and s_2 are guessed systematically and **Eq. (4.5.1)** are then integrated numerically as initial value problem until the given boundary conditions at y =1 are satisfied. For each set of parameter values for λ, β, G and γ, the procedure is repeated until conditions at the y = 1 (i.e. $x_1(1) = 0$, $x_2(1) = 0$) are satisfied and the desired degree of accuracy (namely 10^{-7}) of the results obtained is achieved.

4.6. Entropy Analysis

Flow and heat transfer processes between two parallel plates are irreversible. The non-equilibrium conditions arise due to the exchange of energy and momentum within the fluid and at solid boundaries, thus resulting in entropy generation. Apart of the entropy production is due to the heat transfer in the direction of finite temperature gradients and

the other part of entropy production arises due to the fluid friction. The general equation for the entropy generation per unit volume is given by [9, 10, 42 - 47],

$$S^m = \frac{k}{T_w^2}\left(\nabla \bar{T}\right)^2 + \frac{\bar{\mu}}{T_w}\Phi . \qquad \textbf{(4.6.1)}$$

The first term in equation **(4.4.3)** is the irreversibility due to heat transfer and the second term is the entropy generation due to viscous dissipation. Using equation **(4.6.1)**, we express the entropy generation number in dimensionless form as,

$$Ns = \frac{H^2 E^2 S^m}{kR^2 T_w^2} = \left(\frac{\partial T}{\partial y}\right)^2 + \frac{\mu Br}{\beta}\left(\frac{\partial u}{\partial y}\right)^2 + O(\varepsilon^2), \qquad \textbf{(4.6.2)}$$

In equation **(4.6.2)**, the first term can be assigned as N_1 and the second term due to viscous dissipation as N_2, i.e.

$$N_1 = \left(\frac{\partial T}{\partial y}\right)^2, \quad N_2 = \frac{\mu Br}{\beta}\left(\frac{\partial u}{\partial y}\right)^2 . \qquad \textbf{(4.6.3)}$$

In order to have an idea whether fluid friction dominates over heat transfer irreversibility or vice-versa, Bejan [1, 2] defined the irreversibility distribution ratio as $\Phi = N_2/N_1$. Heat transfer dominates for $0 \leq \Phi < 1$ and fluid friction dominates when $\Phi > 1$. The contribution of both heat transfer and fluid friction to entropy generation are equal when $\Phi = 1$. In many engineering designs and energy optimisation problems, the contribution of heat transfer entropy N_1 to overall entropy generation rate Ns is needed. As an alternative to irreversibility parameter, the Bejan number (Be) is define mathematically as

$$Be = \frac{N_1}{Ns} = \frac{1}{1+\Phi} \ . \qquad \textbf{(4.6.4)}$$

Clearly, the Bejan number ranges from 0 to 1. *Be* = 0 is the limit where the irreversibility is dominated by fluid friction effects and *Be* = 1 corresponds to the limit where the irreversibility due to heat transfer by virtue of finite temperature differences dominates. The contribution of both heat transfer and fluid friction to entropy generation are equal when *Be* = 1/2.

4.7. Results and Discussion

In this section, we validate the above theoretical results using physically realistic values of various embedded parameters in the numerical experiment. It is important to note that increasing parameter value of β indicates an increase in the fluid viscosity and a decrease in the fluid activation energy. Also the reactive flow Arrhenius kinetics increases whenever the parameter value of λ increases. A comparison between the results obtained using perturbation technique and purely fourth-order Runge–Kutta numerical integration coupled with shooting method at small and moderate parameter values are shown in **Table 4.7.1.** Generally, the difference is of order 10^{-8} and a perfect agreement is noticed.

Table 4.7.1: Comparison between analytical and numerical results ($\beta = 0.1$, $\lambda=0.1$, $\gamma =1$)

y	$T(y)$ Perturbation Results	$T(y)$ Numerical Results	$\left\|T_{numer.} - T_{perturb.}\right\|$
0	0.0613101824	0.0613102561	$7.37\text{x}10^{-8}$
0.1	0.0607779277	0.0607779882	$6.05\text{x}10^{-8}$
0.2	0.0591711058	0.0591711735	$6.77\text{x}10^{-8}$
0.3	0.0564596206	0.0564596904	$6.98\text{x}10^{-8}$
0.4	0.0525935701	0.0525936349	$6.48\text{x}10^{-8}$
0.5	0.0475036426	0.0475037015	$5.89\text{x}10^{-8}$
0.6	0.0411016883	0.0411017440	$5.57\text{x}10^{-8}$
0.7	0.0332814815	0.0332815254	$4.39\text{x}10^{-8}$
0.8	0.0239196931	0.0239197333	$4.02\text{x}10^{-8}$
0.9	0.0128770923	0.0128771399	$4.76\text{x}10^{-8}$
1.0	0	0	0

In order to obtain the thermal stability criterion in the flow system, the Hermite-Padé approximation procedure in **section (4.4)** above was applied to the first few terms of the solution series in **section (4.2)** and we obtained the results as shown in **tables (4.7.2)** and **(4.7.3)** below:

Table 4.7. 2: Computations showing the criticality procedure rapid convergence ($\beta = 0$, $\gamma = 1$).

d	N	Nu	λ_{cN}
2	4	2.150123257	0.7583073286
3	8	2.250048451	0.7697232875
4	13	2.250005672	0.7697210224
5	19	2.250005680	0.7697210227
6	26	2.250005680	0.7697210227

Table 4.7.3: Computations showing thermal criticality for different parameter values

β	γ	Nu	λ_c
0	1.0	2.25000568	0.769721022
0.1	1.0	2.85858464	0.86686845
0.2	1.0	4.34187920	1.02124670
0.1	0.5	2.70916381	0.92391437
0.1	0.3	2.64469729	0.94869368
0.1	0.1	2.57732112	0.97470948

The results in table **(4.7.2)** reveal the rapid convergence of Hermite-Padé approximation procedure with gradual increase in the number of series coefficients utilized in the approximants. In **table (4.7.3)**, it is noteworthy that the magnitude of thermal criticality (λ_c) increases with a decrease in the reactive flow activation energy and an increase in the fluid viscosity (i.e. $\beta > 0$). This invariably will lead to a delay in the development of thermal runaway in the flow system and enhance flow thermal stability. An increase in the viscous heating (i.e. $\gamma > 0$) causes a decrease in the magnitude of thermal criticality parameter, leading to early development of thermal ignition in the system.

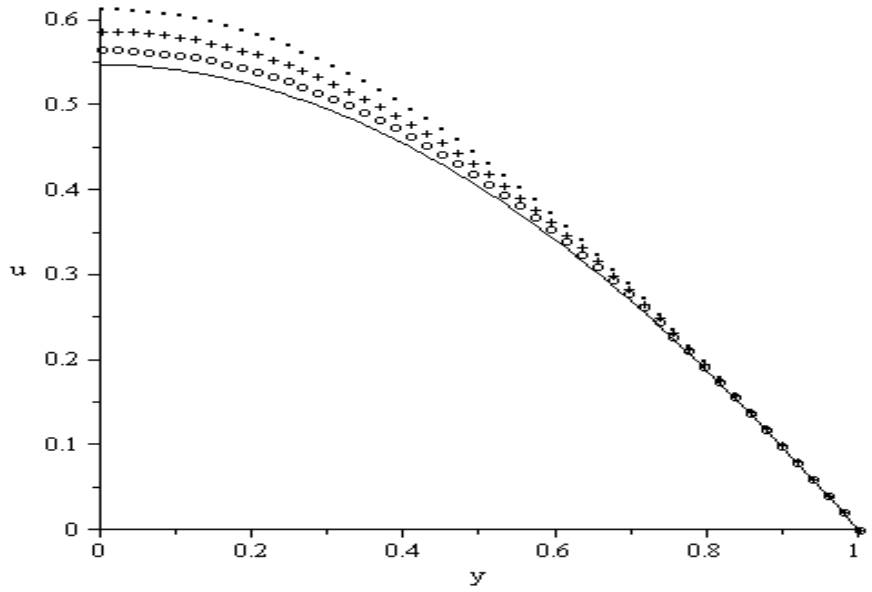

Fig.4.7.1. Velocity profile: β = 0.1; G = 1; Br = 1; _____ λ =0.1; oooooλ = 0.2; ++++ λ = 0.3; ……λ = 0.4.

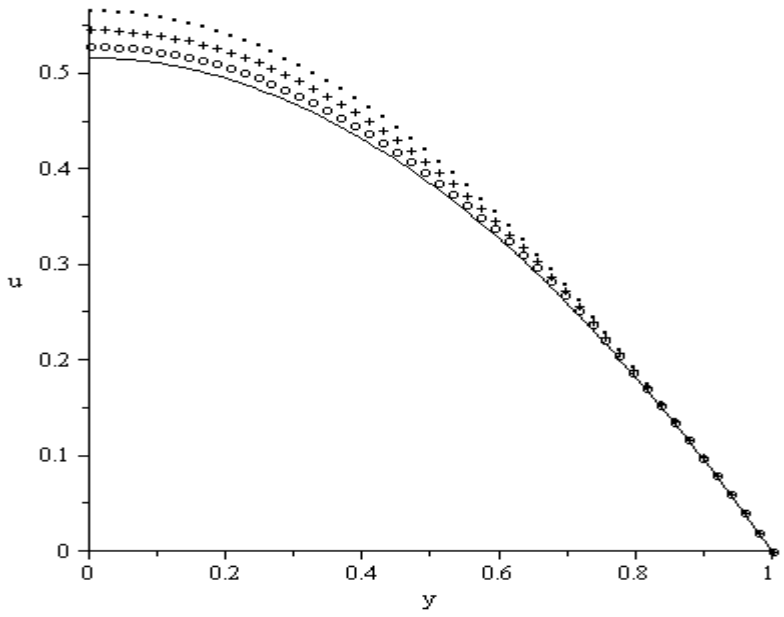

Fig.4.7.2. Velocity profile: β = 0.1; G = 1; λ = 0.1; _____*Br* = 0.1; ooooo*Br* = 0.5; ++++*Br* = 1; ……..*Br* = 1.5.

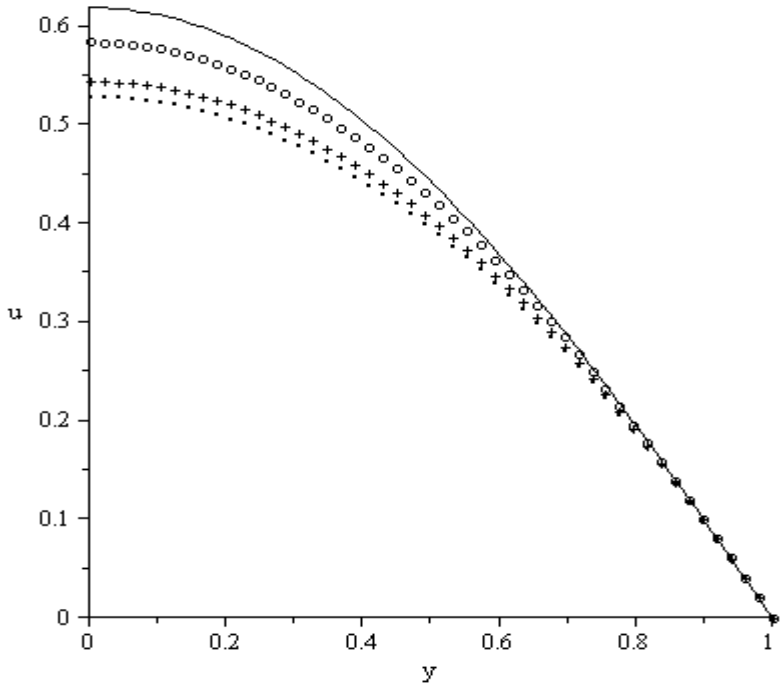

Fig.4.7.3. Velocity profile: G = 1; Br = 1; λ = 0.4*;* _____β = 0; oooooβ= 1; ++++β = 5; …....β = 10.

The velocity profiles are reported for increasing values of λ, γ and β in **Figs. (4.7.1-4.7.3)**. The fluid velocity is zero at the walls and increases gradually towards the channel centreline. For $\lambda = 0$, the fluid shows the standard Poiseuille parabolic velocity profile with maximum velocity along the channel centreline. As the parameter value of $\lambda > 0$ increases, the Arrhenius kinetic increases, causing the fluid velocity in the channel core region to further increase as shown in **Fig. 4.7.1**. Similar trend is observed in **Fig. 4.7.2**. The velocity profile increases with increase in the Brinkman number *Br* due to viscous heating. Moreover, in **Fig. 4.7.3** the fluid velocity in the channel core region decreases as the value of β increases due to a decrease in the fluid activation energy and an increase in the fluid viscosity.

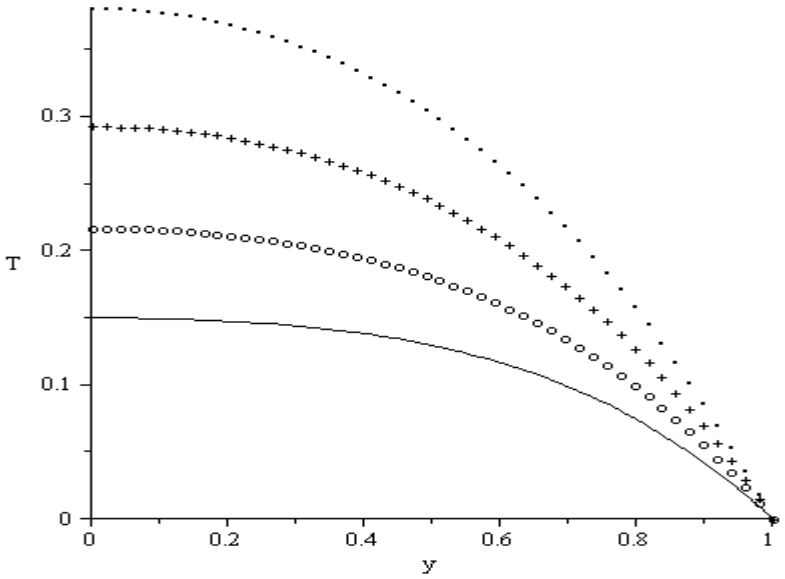

Fig.4.7.4. Temperature profile: β = 0.1; G=1; Br=1; _____ λ = 0.1; oooooλ = 0.2; ++++ λ = 0.3; ……λ = 0.4.

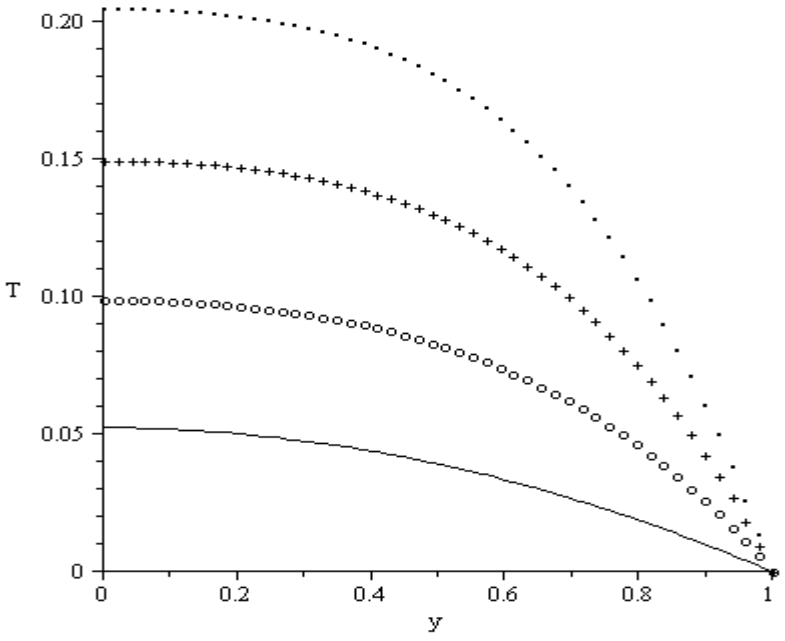

Fig. 4.7.5. Temperature profile: β = 0.1; G = 1; λ = 0.1; _____*Br* = 0.1; ooooo*Br* = 0.5; ++++*Br* = 1; …....*Br* = 1.5.

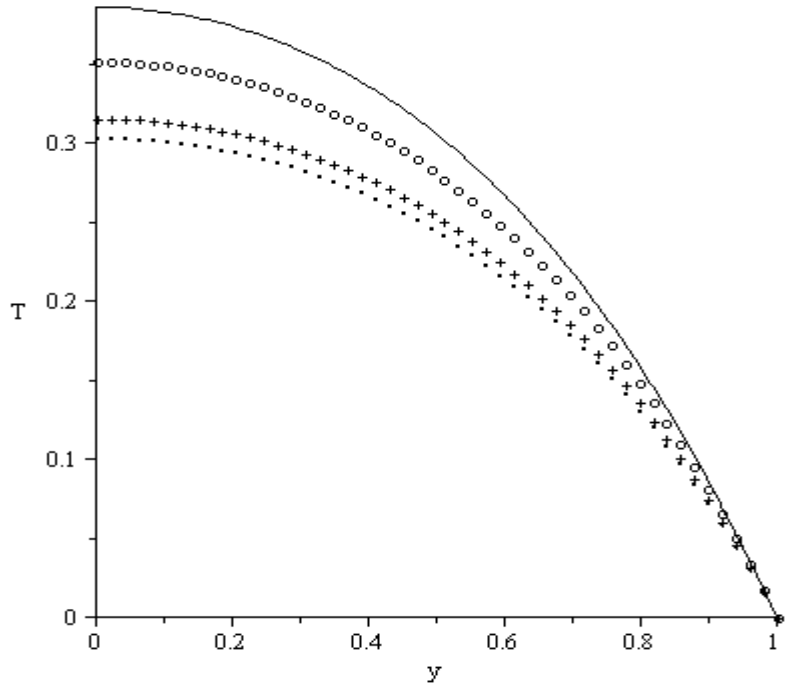

Fig. 4.7.6. Temperature profile: G = 1; Br = 1; λ = 0.4; _____β = 0; oooooβ= 1; ++++β = 5; …....β = 10.

Typical variations of the fluid temperature profiles in the normal direction are shown in **Figs. (4.7.4 - 4.7.6)**. An increase in the parameter values of λ and Br causes a further increase in the fluid temperature. This can be attributed to an increase in heat generation within the fluid due to combine action of exothermic reaction and viscous heating as illustrated in **Figs. (4.7.4 - 4.7.5)**. A decrease in the fluid temperature is observed when the parameter value of β increases, in this case, the fluid activation energy is reduced and its viscosity has increased **(Fig. 4.7.6)**. Meanwhile, minimum temperature is generally observed at the channel walls while the maximum temperature occurs around the core region of the channel.

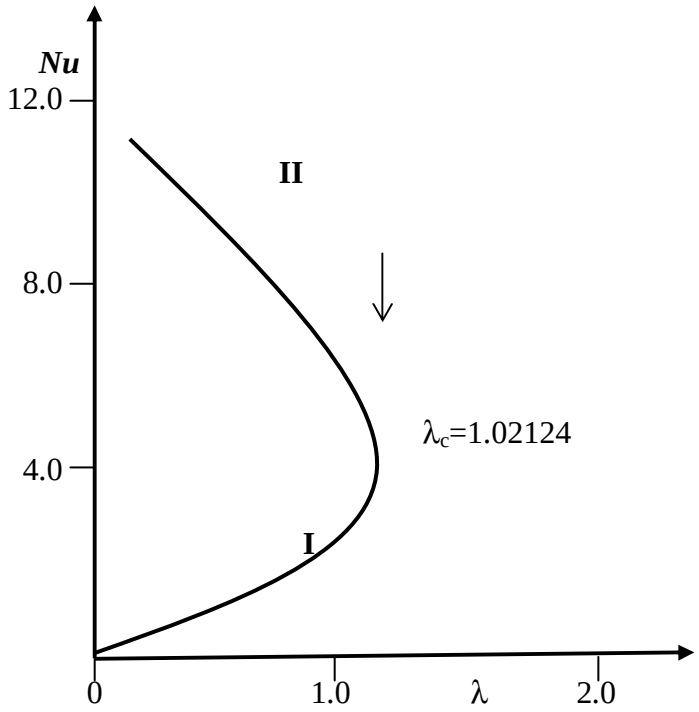

Fig. 4.7.7. A slice of approximate bifurcation diagram in the (λ , *Nu*(β = 0.2, γ= 1)) plane

A slice of the bifurcation diagram for 0< β << 1 in the (λ, *Nu*) plane is shown in **Fig. 4.7.7**. It represents the qualitative change in the flow system as the parameter (λ) increases. In particular, for 0≤β <<1 and γ >0 there is a critical value λ_C (a turning point) such that, for $0 < \lambda < \lambda_c$ there are two solutions **(labelled I and II)**. The upper and lower solution branches occur due to the nonlinearity in the temperature dependent variable viscosity and Arrhenius kinetics in the governing thermal boundary layer **Eq. (4.2.13)**. When $\lambda > \lambda_C$ the system has no real solution and displays a classical form indicating thermal runaway. As temperature increases, the fluid viscosity decreases exponential and the exothermic reaction due to Arrhenius kinetics increases. The velocity gradient specified by **Eq. (4.2.13)**, increases exponentially with temperature coupled with increasing Arrhenius kinetics and feeds back into the temperature equation, leading to thermal runaway [33, 52, 60].

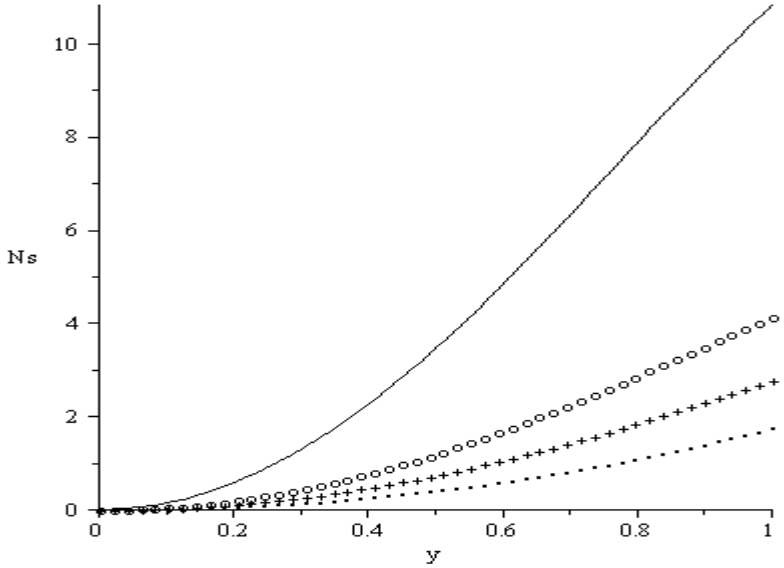

Fig. 4.7.8. Entropy generation rate: G= 1; Br = 1; λ=0.4; _____β = 0.1; ooooo β= 0.3; ++++ β = 0.5; …...β = 1.

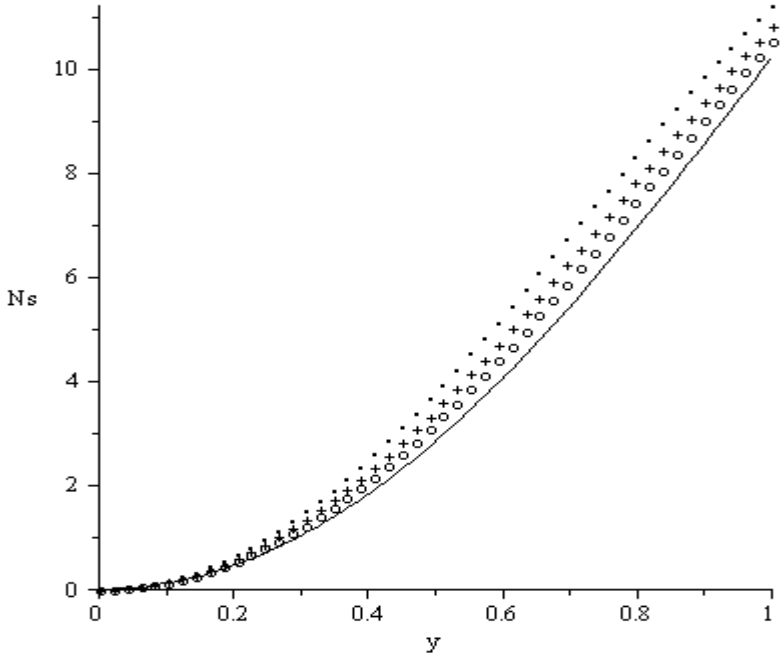

Fig. 4.7.9. Entropy generation rate: β = 0.1; G= 1; Br = 1; _____ λ = 0.1; oooooλ = 0.3; ++++ λ = 0.4; ……λ = 0.5.

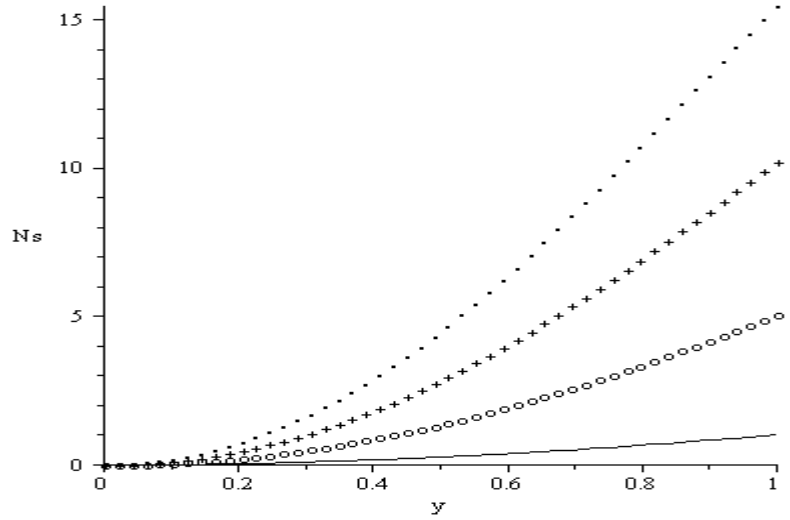

Fig. 4.7.10. Entropy generation rate: $\beta = 0.1$; G = 1; $\lambda = 0.1$; _____*Br* = 0.1; ooooo*Br* = 0.5; ++++*Br* = 1; ….....*Br* = 1.5.

Figs. (4.7.8 - 4.7.10) display results for the entropy generation versus the channel half width for various parametric values. Generally, entropy generation rate is maximum at the channel walls and minimum at the core region of the channel. It is interesting to note that the entropy generation rate decreases with increasing value β and increases with increasing value of λ and Br. Hence, an increase in the both Arrhenius kinetics and viscous heating in the flow system may lead to a decrease in the thermodynamic performance of the system.

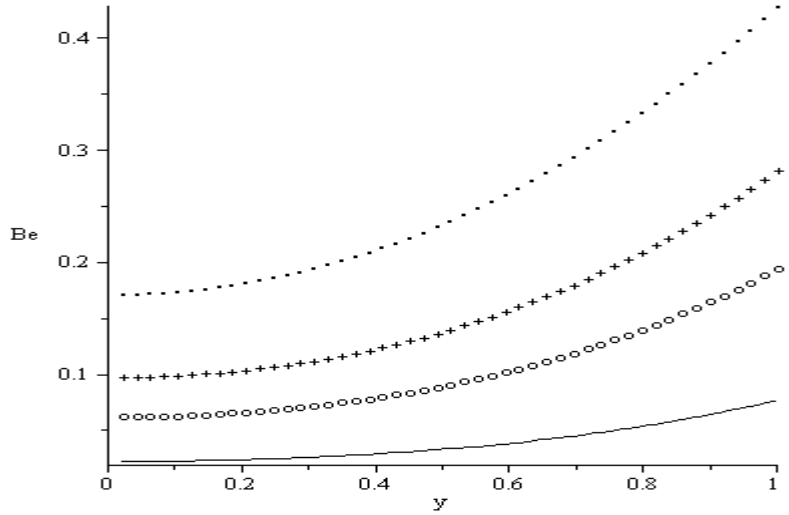

Fig. 4.7.11. Bejan number: G= 1; Br = 1; λ*=0.4;* ____β = 0.1; oooooβ= 0.3; ++++ β = 0.5; …...β = 1.

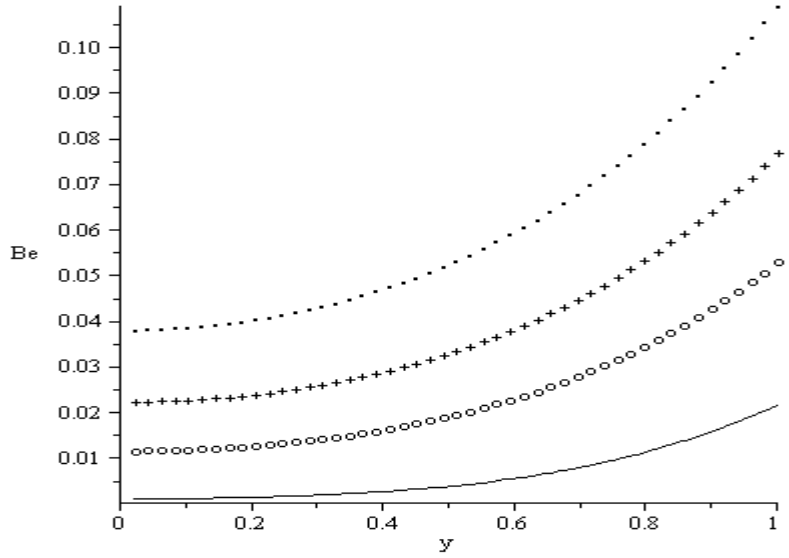

Fig. 4.7.12. Bejan number: β = 0.1; G= 1; Br = 1; _____ λ = 0.1; oooooλ = 0.3; ++++ λ = 0.4; ……λ = 0.5.

Figs. (4.1.7.11 - 4.1.7.12) display the Bejan (*Be*) number versus the channel half width. It is observed that the fluid friction irreversibility dominates at the channel core region while the heat transfer irreversibility dominates at the walls. The dominant effect of heat transfer irreversibility in the flow system increases with increasing values of β and λ.

CHAPTER

5

CONCLUDING REMARKS

In this thesis, we investigate the heat transfer and entropy generation rate in a reactive variable viscosity channel flow. The evaluation of the entropy production rates for variable viscosity reactive Couette flow was carried out using both analytical and numerical techniques in **Chapter 3**. Solutions are obtained for fluid velocity and temperature profiles. Using a special type of Hermite-Padé approximation technique, we obtain accurately the thermal criticality conditions and the solution branches. The volumetric entropy generation rate and the Bejan number depend on fluid viscosity variation and activation energy parameter (β) and heat generation parameter (γ). Our results reveal that for all parametric values, fluid friction irreversibility dominates at the channel core region while at both lower fixed and upper moving plate surfaces the heat transfer irreversibility dominates.

In **chapter 4**, the evaluation of the entropy production rates for variable viscosity reactive Poiseulle flow was carried out using both analytical and numerical techniques. Solutions are obtained for fluid velocity and temperature profiles. Using a special type of Hermite-Padé approximation technique, we obtain accurately the thermal criticality conditions and the solution branches. The volumetric entropy generation rate and the Bejan number depend on fluid viscosity variation and activation energy parameter (β), Frank-Kamenetskii parameter (λ) and the Brinkman number (Br). Our results reveal that for all

parametric values, fluid friction irreversibility dominates at the channel core region while at walls the heat transfer irreversibility dominates.

Finally, for both Couette and Poiseuille flow models considered, the thermodynamic performance of the flow systems can be enhanced by appropriately choosing the values of the embedded parameters controlling the flow systems

5.2 FURTHER WORK

These problems have been looked at as 1 dimensional problems, so future work one can look at them as two dimensional problems.

BIBLIOGRAPHY

[1] H. I. Andersson, De-Yi Shang. An extended study of the hydrodynamics of gravity-driven film flow of power law fluids. Fluid Dynamics Research, 22, 345 (1998).

[2] J. Adler. Thermal explosion theory for reactive flow between parallel heated walls. Combustion and Flames 24, 151-158, (1975).

[3]G. W. Andrew. Stability of circular Poiseuille-Couette flow to asymmetry disturbances. Journal of Fluid Mechanics 500, 169-210, (2004).

[4] M. Ayub, A. Rasheed, T. Hayat. Exact flow of a third grade fluid past a porous plate using homotopy analysis method. Int. J. Eng. Sci. 41, 2091, (2003).

[5] A. Aziz, T. Y. Na. Perturbation Methods in Heat Transfer. Hemisphere Publishing Corporation, Washington, New York, (1984).

[6] A. Aziz. Entropy generation in pressure gradient assisted Couette flow with different thermal boundary conditions. Entropy 8 50–62, (2006).

[7] A. Abu-Hijleh. Natural convection and entropy generation from a cylinder with high conductivity fins. Numer. Heat Transfer A 39 405–32, (2004).

[8] G. K. Batchelor. An introduction to fluid dynamics. Cambridge University Press, (1967).

[9] A. Bejan. Entropy generation through heat and fluid flow. Canada: Wiley, 98, (1994).

[10] A. Bejan. Entropy generation minimization. Boca Raton, FL: CRC Press, (1996).

[11] V. Berdichevsky, A. Fridlyand, V.Sutyrin. Prediction of turbulent velocity profile in Couette and Poiseuille flows from first principles. The American Physical Society, 21 (76), 3967-3970, (1996).

[12] J. B Boxall, I. Guymer, A. Marion. Transverse mixing in sinuous open channels. J. of Hydraulic Research, 41(2):153-165, (2003).

[13] S. A. Blair. Reynolds-Ellis equation for line contact with shear- thinning. Tribology, 1-7, (2005).

[14] R. B. Bird, W. E. Stewart, E. N. Lightfoot. Transport phenomenon. John Wiley & Sons, (1960).

[15] A. G. Carrington, Z. F. Sun. Second law analysis of combined heat and mass transfer in internal and external flows. Int. J. Heat Fluid Flow 13 65–70, (1992).

[16] Y. A Cengel, M. A. Boles. Thermodynamics: An engineering approach. McGraw-Hill, New York, (2001).

[17] R. P. Chhabra, J. F. Richardson. Non-Newtonian flow in the process industries. Butterworth Heinemann, (1999).

[18] K. E. Chin, R. Nazar, N. M. Arifin, I. Pop. Effect of variable viscosity on mixed convection boundary layer flow over a vertical surface embedded in a porous medium. International Communication in Heat and Mass Transfer 34, 464-473, (2007).

[19] A. Costa, G. Macedonio. Viscous heating in fluids with temperature- dependent viscosity: implications for magma flows. Nonlinear Processes in Geo- physics 10, 545-555, (2003).

[20] A. Costa, G. Macedonio. Viscous heating effects in fluids with temperature-dependent viscosity: triggering of secondary flows. Journal of fluids Mechanics 540, 21-38, (2005).

[21] K. Darko, S. Vladimir. Mathematical modeling of changing of dynamic viscosity, as a function of temperature and pressure, of mineral oils for hydraulic systems. FACTAS Universitatis, Mechanical Engineering series 4 (1), 27-34, (2006).

[22] S. H. Davis, G. A. Griegsmann, R. L. Laurence, S. Rosenblat. Multiple solutions and hysteresis in steady parallel viscous flows. Physics of Fluids 26, 1177-1182, (1983).

[23]J. F. Douglas, J. M. Gasiorek, J. A. Swaffield. Fluids Mechanics. Addison Wesley Longman Ltd., Harlow, (1995).

[24] A. Dwight, L. S. Tuckerman. Stability analysis of perturbed plane Couette flow. Physics of Fluids 11 (5), 1187-1195, (1999).

[25] B. Fantino, M. Godet, J. Frene. Studies of engine bearings and lubrication. Society of Automotive Engineers Special Publication 539, 23-32, (1983).

[26] J. Feng, L. G. Leal. Pressure driven channel flows of a model liquid-crystalline polymer. Phys., of Fluids. Vol., 11, No. 10, 2821-2835, (1999).

[27] R. L. Fosdick, K. R. Rajagopal. Thermodynamics and stability of fluids of third grade. Proc. Roy. Soc. London A, 339, 351, (1980).

[28] J. H. He, X. H. Wu. Variational iteration method: New development and applications, computers & mathematics with applications, 54(7-8), 881-894, (2007).

[29] J. H. He. Variational iteration method - Some recent results and new interpretations, J. Computational and Applied Mathematics, 207 (1), 3-17, (2007).

[30] J. H. He, X. H. Wu. Construction of solitary solution and compacton-like solution by variational iteration method, Chaos Solitons & Fractals, 29 (1), 108-113, (2006).

[31] J. H. He. Some asymptotic methods for strongly nonlinear equations, Int. J. Modern Phys. B 20 (10), 1141–1199, (2006).

[32] S. J. Hyder, B. S. Yilbas. Entropy analysis of conjugate heating in a pipe flow Int. J. Energy Res. 26 253–262, (2002).

[33] G. Ibanez, S. Cuevas, H. Lopez de Haro. Minimization of entropy generation by asymmetric convective cooling Int. J. Heat Mass Transfer. 46 ,1321–1328, (2003).

[34] W. M Kays, M. E. Crawford. Convective heat and mass transfer. Mcgraw-Hill, Inc., (1993).

[35] M. Inokuti, H. Sekine, T. Mura. General use of the Lagrange multiplier in nonlinear mathematical physics. In: Nemat-Nassed S, editor. Variational method in the mechanics of solids. Pergamon press, 156–162, (1978).

[36] O. D. Makinde. Computer extension and bifurcation study by analytic continuation of porous tube flow. Jour. Math. Phys. Sci. Vol. 30, 1-24, (1996).

[37] O. D. Makinde. Steady flow in a linearly diverging asymmetrical channel. Comp. Assist. Mech. Eng. Sc. Vol. 4, 157-165, (1997).

[38] O. D. Makinde. Extending the utility of perturbation series to problems of laminar flow in a porous and a diverging tube. Jour. Australian Math. Soc. Series B, Vol. 41, 118-128, (1999).

[39] O. D. Makinde, P. Sibanda. Steady flow in a diverging symmetrical channel: Numerical study of Bifurcation by analytic continuation. Quaestiones Mathematicae, Vol. 23, 45-57, (2000).

[40] O. D. Makinde, P. Sibanda. Fluid dynamics of the sliding plate. Quaestiones Mathematicae, Vol. 23, 59-66, (2000).

[41] O. D. Makinde. Laminar falling liquid film with variable viscosity along an inclined heated plate. Applied Mathematics and Computation, Vol. 175, 80-88, (2006).

[42] O. D. Makinde. Irreversibility analysis for gravity driven non-newtonian liquid film along an inclined isothermal plate Phys. Scr. 74, 642–645, (2006).

[43] O. D. Makinde. Hermite–Padé approximation approach to steady flow of a liquid film with adiabatic free surface along an inclined heat plate Physica A 381 1–7, (2007).

[44] O. D. Makinde. Thermal ignition in a reactive viscous flow through a channel filled with a porous medium. ASME, Journal of Heat Transfer – Vol. 128,601-604, (2006).

[45] O. D. Makinde. Irreversibility analysis of variable viscosity channel flow with convective cooling at the walls. 86, 383–389, (2008).

[46] O. D. Makinde. Entropy-generation analysis for variable-viscosity channel flow with non-uniform wall temperature. Applied Energy, Vol. 85, 384-393, (2008).

[47] O. D. Makinde, R. L. Maserumule. Thermal criticality and entropy analysis for variable viscosity Couette flow. Physica Scripta, Vol. 78, 015402 (6pp) (2008).

[48] M. Massoudi, I. Christe. Effects of variable viscosity and viscous dissipation on the flow of a third grade fluid in a pipe. Int. J. Non-Linear Mech. 30, 687, (1995).

[49] U. Narusawa. The second law analysis of mixed convection in rectangular ducts. Heat Mass Transfer 37 197–203, (2001).

[50] G. P. Roberts, H. A. Barnes, P. Carew. Modelling the flow of very shear thinning liquids. Chem., Eng., Sci., 56, 5617-5623, (2001).

[51] K. R. Rajagopal. On boundary conditions for fluids of the differential type. In: Sequira A. editor. Navier-Stokes equations and related non-linear problems. New York: Plenum press, 273, (1995).

[52] A. Z. Sahin. Effect of variable viscosity on the entropy generation and pumping power in a laminar fluid flow through a duct subjected to constant heat flux heat mass transfer 35. 499–506, (1999).

[53] S. H. Tasnim, S. Mahmud. Entropy generation in a vertical concentric channel with temperature dependent viscosity. Int. Commun. Heat Mass Transfer 29 907–918, (2002).

[54] S. K. Wilson, B. R. Duffy. Strong temperature dependent viscosity effects on a rivulet draining down a uniformly heated or cooled slowly varying substrate. Phys. of Fluids, Vol., 15, No. 4, 827-840, (2003).

[55] F. M. White. Viscous fluid flow, 3rd Edition. McGraw-Hill, Inc., (2006).

[56]M. Yurusoy, M. Pakdemirli. Approximate analytical solutions for the flow of a third grade fluid in a pipe. Int. J. Non-Linear Mech. 37, 187, (2002).

[57]L. C. Zheng, X. X. Zhang. Skin friction and heat transfer in power-law fluid laminar boundary layer along a moving surface. Int., J., Heat and Mass Transfer, 45(35), 2667 - 2672, (2002).

[58] P. C. Bowes, Self-heating: Evaluating and Controlling the Hazard. Elsevier, Amsterdam, (1984).

[59] D. A. Frank Kamenetskii, Diffusion and heat transfer in chemical kinetics. Plenum Press, (1969).

[60] H. Schlichting, Boundary layer theory, Springer-Verlag, New York, (2000).

[61] R. I. Tanner, Engineering Rheology, Oxford Science Publications, 1985.

[62] S. Yasutomi, S. Bair, W. O. Winer, An application of a free volume model to lubricant rheology. 1. Dependence of viscosity on temperature and pressure, Trans. ASME J. Tribol. 106 (2) (1984) 291–303.

[63] http://maplesoft.com/products/maple/technical.aspx

[64] C. Bender, and S. A. Orszag, Advanced mathematical methods for scientists and engineers, McGraw-Hill, (1978).

[65] A. J. Guttamann, Asymptotic analysis of power series expansions, Phase Transitions and Critical Phenomena, C. Domb and J. K. Lebowitz, eds. Academic Press, New York, (1989) 1-234.

[66] R. S. Reddy Gorla, L. W. Byrd, D. M. Pratt, Second law analysis for microscale flow and heat transfer, Applied Thermal Engineering, Vol. 27, (2007) 1414-1423.

[67] B. N. Taufiq, H. H. Masjuki, T. M. I. Mahlia, R. Saidur, M. S. Faizul, E. Niza Mohamad, Second law analysis for optimal thermal design of radial fin geometry by convection, Applied Thermal Engineering, Vol. 27, (2007) 1363-1370.

[68] A. Bejan, Entropy generation through heat and fluid Flow, John Wiley & Sons. Inc.: Canada, Chapter 5, p98 (1994).

[69] A. Bejan, Entropy generation minimization, CRC Press, Boca Raton, Florida, (1996).

[70] G. Ibanez, S. Cuevas, M. Lopez de Haro, Minimization of entropy generation by asymmetric convective cooling, Int. J. Heat Mass Transfer, Vol. 46, (2003) 1321-1328.

[71] W. M. Kays, M. E. Crawford, Convective heat and mass transfer, McGraw-Hill, (1980).

[72] O. D. Makinde, Irreversibility analysis for gravity driven non-Newtonian liquid film along an inclined isothermal plate, Physica Scripta, Vol. 74, (2006) 642-645.

[73] O. D. Makinde, Hermite-Padé approximation approach to steady flow of a liquid film with adiabatic free surface along an inclined heat plate, Physica A, Vol. 381, (2007) 1-7.

[74] U. Narusawa, The second law analysis of mixed convection in rectangular ducts, Heat and Mass Transfer, 37 (2001) 197-203.

[75] A. Z. Sahin, Effect of variable viscosity on the entropy generation and pumping power in a laminar fluid flow through a duct subjected to constant heat flux, Heat Mass Transfer, 35, (1999) 499-506.

[76] S. H. Tasnim, S. Mahmud, Entropy generation in a vertical concentric channel with temperature dependent viscosity, Int. Comm. Heat Mass Transfer, Vol. 29, No. 7, (2002) 907-918.

[77] M. M. Vainberg, V. A. Trenogin, Theory of branching of solutions of nonlinear equations, Noordoff, Leyden, USA (1974).

[78] L.E. Johns, R. Narayanan. Frictional heating in plane Couette flow. Proc. Roy. Soc. A 453, 1653–1670 (1997).